STEM CELLS AND DEVELOPMENT
Volume 24, Number 23, 2015

DOI: 10.1089/scd.2015.0153

Cultured Human Adipose Tissue Pericytes and Mesenchymal Stromal Cells Display a Very Similar Gene Expression Profile

Lindolfo da Silva Meirelles,[1,2] Tathiane Maistro Malta,[1] Virgínia Mara de Deus Wagatsuma,[1] Patrícia Viana Bonini Palma,[1] Amélia Goes Araújo,[3] Kelen Cristina Ribeiro Malmegrim,[4] Fábio Morato de Oliveira,[1] Rodrigo Alexandre Panepucci,[3] Wilson Araújo Silva Jr.,[1,5] Simone Kashima Haddad,[1] and Dimas Tadeu Covas[1,6]

Mesenchymal stromal cells (MSCs) are cultured cells that can give rise to mature mesenchymal cells under appropriate conditions and secrete a number of biologically relevant molecules that may play an important role in regenerative medicine. Evidence indicates that pericytes (PCs) correspond to mesenchymal stem cells in vivo and can give rise to MSCs when cultured, but a comparison between the gene expression profiles of cultured PCs (cPCs) and MSCs is lacking. We have devised a novel methodology to isolate PCs from human adipose tissue and compared cPCs to MSCs obtained through traditional methods. Freshly isolated PCs expressed CD34, CD140b, and CD271 on their surface, but not CD146. Both MSCs and cPCs were able to differentiate along mesenchymal pathways in vitro, displayed an essentially identical surface immunophenotype, and exhibited the ability to suppress $CD3^+$ lymphocyte proliferation in vitro. Microarray expression data of cPCs and MSCs formed a single cluster among other cell types. Further analyses showed that the gene expression profiles of cPCs and MSCs are extremely similar, although MSCs differentially expressed endothelial cell (EC)-specific transcripts. These results confirm, using the power of transcriptomic analysis, that PCs give rise to MSCs and suggest that low levels of ECs may persist in MSC cultures established using traditional protocols.

Introduction

Mesenchymal stem cells are defined as cells able to self-renew and give rise to a number of cell types characteristic of mesenchymal tissues [1]. Since most works on this cell type use cultured cells operationally defined as mesenchymal stem cells because of their adherence to plastic, proliferation, and differentiation in vitro without clear evidence of their self-renewal in vivo, the term multipotent mesenchymal stromal cell (MSC) has been proposed to be more appropriate to describe these cultured cells [2]. The differentiation capabilities of MSCs make their use interesting for tissue engineering [3]. MSCs may also be important in regenerative medicine owing to their trophic and immunomodulatory properties [4].

A recurrent question regarding MSCs concerns their in vivo origins, that is, which cells give rise to MSC cultures? Various types of evidence indicate that pericytes (PCs), cells that wrap around endothelial cells (ECs) in blood vessels, are the best candidates [5]. One way to answer the question above would be to isolate PCs and culture them as MSCs to see if the characteristics of both cell populations match.

PC-associated molecules [6] could be used to select PCs, but their expression does not always distinguish PCs from other cells. For example, the use of CD146 as a marker for PC isolation may provide a cell population that contains not only PCs but also ECs and smooth muscle cells, which also express this molecule [7]. Even when CD146 was combined with other marker molecules to isolate PCs, the resulting cell population still could not be considered free of cells from the tunica adventitia of blood vessels [8].

In view of the above, we sought to circumvent some of the problems related to PC isolation by using a functional

[1]Center for Cell-Based Therapy (CEPID/FAPESP), Regional Center for Hemotherapy of Ribeirão Preto, University of São Paulo, Ribeirão Preto, Brazil.
[2]Laboratory for Stem Cells and Tissue Engineering, PPGBioSaúde, Lutheran University of Brazil, Canoas, Brazil.
[3]Laboratory of Large-Scale Functional Biology (LLSFBio), Regional Center for Hemotherapy of Ribeirão Preto, University of São Paulo, Ribeirão Preto, Brazil.
[4]School of Pharmaceutical Sciences of Ribeirão Preto, Universidade de São Paulo, Ribeirão Preto, Brazil.
Departments of [5]Genetics and [6]Clinical Medicine, School of Medicine of Ribeirão Preto, University of São Paulo, Ribeirão Preto, Brazil.

selection criterion, namely the ability to adhere to tissue culture-treated plastic surfaces, in addition to expression of a PC surface maker and the absence of expression of an EC surface molecule. Adipose tissue (AT) was chosen as the source of cells because its stromal–vascular fraction (SVF), which contains PCs and can give rise to cultured MSCs, can be easily separated from parenchymal cells by centrifugation after enzymatic disaggregation [9]. The PC marker chosen was the antigen defined by the 3G5 antibody [10,11]. This antigen has been reported to be present in perivascular cells in human AT and, additionally, to yield the highest number of fibroblastic colonies when used as a marker for positive cell selection compared with CD146 or the antigen defined by the STRO-1 antibody [12]. The marker chosen for negative selection was CD31, which is constitutively expressed on the surface of ECs and some leukocytes [13].

We refer to the $3G5^+CD31^-$ cell population isolated by us as AT-derived $3G5^+$ cells (AT3G5Cs). AT3G5Cs were confirmed to be periendothelial in situ. Culture-expanded AT3G5Cs (cAT3G5Cs) were subjected to characterization procedures in parallel with AT-derived MSCs (ATMSCs) that were isolated and cultured using traditional methods. cAT3G5Cs exhibited MSC characteristics such as a typical surface molecule profile, in vitro differentiation capability, and ability to suppress $CD3^+$ lymphocyte proliferation in vitro. Clustering analyses of the gene expression profiles of cAT3G5Cs and ATMSCs showed that these two cell types form a single distinct cluster among other cell types. Further analyses indicated that the number of molecules differentially expressed by cAT3G5Cs and ATMSCs is relatively small and is probably related to the persistence of a small amount of ECs in ATMSC cultures.

Materials and Methods

Reagents and materials

General reagents, culture media, and saline solutions used in this study were purchased from Sigma-Aldrich Brasil Ltda (São Paulo, Brazil), unless specified otherwise. Fetal bovine serum (FBS) was acquired from Hyclone (GE Healthcare Life Sciences, Logan, UT). Plasticware used was supplied by Greiner Bio-One Brasil Produtos Medicos Hospitalares Ltda (Americana, Brazil). PC medium (PM) was obtained from ScienCell Research Laboratories (Carlsbad, CA).

Enzymatic disaggregation of human AT

Human AT was obtained as discarded material from liposuction or postbariatric dermolipectomy surgeries at the University Hospital of the School of Medicine of Ribeirão Preto, University of São Paulo (HCFMRP-USP), after informed consent from the patients. The Brazilian National Commission on Ethics in Research (CONEP) has approved the use of tissue samples from human subjects described in this work (CAAE 0054.0.004.000-08). All tissue donors who agreed to participate in this study provided written informed consent. A description of AT samples and donor characteristics is shown in Table 1.

Using a wide bore pipette, liposuction material was dispensed into 50-mL centrifuge tubes ($\sim$30 mL per tube), which contained 15 mL of Ca^{2+} and Mg^{2+}-free Hank's balanced salt solution with added 10 mM HEPES (CMF-HBHBSS). Tubes were capped and the contents mixed by inversion. The samples were centrifuged at 600 *g* for 10 min. After removal of the top oily layer with a Pasteur pipette, the buoyant AT fractions were harvested and transferred to fresh 50-mL centrifuge tubes to estimate their volume. When dermolipectomy material was used, subcutaneous AT was cut into small fragments with surgical scissors, and the volume of AT was estimated using a 50-mL centrifuge tube. Two strategies were used for enzymatic digestion, namely direct digestion or two-step digestion.

In the direct digestion strategy, liposuction material was transferred to a polypropylene flask containing an equal volume of collagenase solution [500 U of collagenase I (Worthington Biochemical Corp., Lakewood, NJ) per mL of phosphate-buffered saline (PBS)] and incubated at 37°C for 40 min in a water bath with intermittent swirling of the flask. Dermolipectomy material was enzymatically disaggregated in the same manner, except that the volume of collagenase solution used was twice the volume of AT fragments. At the end of the incubation, the contents of the flask were transferred to 50-mL centrifuge tubes and centrifuged (default centrifugation conditions were 250 *g* for 10 min at room temperature). The pelleted material was resuspended in 15 mL of red blood cell lysis solution [155 mM NH_4Cl, 10 mM $KHCO_3$, 0.1 mM EDTA, 1 mM sodium pyruvate, and 50 U/mL deoxyribonuclease I (DNase I) in ultrapure water]. After incubation for 10 min, the tube was filled with Roswell Park Memorial Institute 1640 medium (RPMI) containing 10% (v/v) FBS (RPMI/10) and centrifuged. The supernatants were discarded, and the pellets were combined and resuspended in RPMI/10. After washing by centrifugation, the pellets were resuspended in RPMI/10, and viable cells were counted using Trypan Blue in a hemocytometer.

The two-step digestion strategy was implemented to increase cell yield and to reduce the absolute amount of collagenase used. Accordingly, AT was mixed with an equal volume (liposuction material) or twice its volume (dermolipectomy material) of RPMI containing 2% FBS (RPMI/2) and 300 U of type I collagenase/mL and incubated at 37°C for 1 h in a polypropylene flask with intermittent swirling. The resulting cell suspension was dispensed into 50-mL centrifuge tubes and centrifuged. The supernatants were discarded, and the pellets were combined and resuspended into RPMI/2. After washing by centrifugation, the pellet was resuspended in 10 mL of RPMI/2 containing 1,000 U/mL of type I collagenase and 30 U/mL of DNase I (Worthington). This cell suspension was incubated at 37°C in a water bath for 40 min to 1 h, with short intervals made to help digestion by pipetting. Remaining cell clumps were removed by filtering with a 100-μm pore cell strainer. After centrifugation and disposal of the supernatant, the pelleted material was resuspended in 15 mL of red blood cell lysis solution and incubated for 10 min. The tube was then filled with RPMI/2 and centrifuged. The pellet was resuspended in RPMI/2, and viable cells were counted with Trypan Blue in a hemocytometer.

Isolation and expansion of ATMSCs

After enzymatic disaggregation, 1×10^6 viable cells were seeded into 100-mm Petri dishes (about 15,000 cells/cm^2) in 7 mL of low-glucose Dulbecco's Modified Eagle's Medium

Table 1. Characteristics of Tissue Donors, Samples, and Cultures Established in This Work

Donor	*Gender*	*Age*	*Surgery type*	*Body site*	*Cultures established*
01	Female	19	Liposuction	Thigh	cAT3G5Cs, ATMSCs
02	Female	41	Liposuction	Thorax, close to the breast	cAT3G5Cs, ATMSCs
03	Female	44	Liposuction	Abdomen	cAT3G5Cs, ATMSCs
04	Female	39	Liposuction	Pool from various sites	cAT3G5Cs, ATMSCs
05	Female	30	Liposuction	Not assessed	cAT3G5Cs, ATMSCs
06	Female	27	Liposuction	Not assessed	cAT3G5Cs, ATMSCs
07	Female	40 (?)	Liposuction	Not assessed	cAT3G5Cs, ATMSCs
08	Female	50	Dermolipectomy	Not assessed	cAT3G5Cs, ATMSCs
09	Male	35	Liposuction	Lower back and flanks	cAT3G5Cs, ATMSCs
10	Female	49	Dermolipectomy	Not assessed	cAT3G5Cs, ATMSCs
11	Female	25	Liposuction	Not assessed	sample used for flow cytometry of fixed cells
12	Female	55	Dermolipectomy	Arms	cAT3G5Cs, ATMSCs
13	Female	29	Dermolipectomy	Not assessed	cAT3G5Cs lost owing to contamination after FACS
14	Female	26	Liposuction	Not assessed	cAT3G5Cs lost owing to contamination after FACS; ATMSCs established
15	Female	39	Liposuction	Not assessed	cAT3G5Cs lost owing to contamination after FACS; ATMSCs established
16	Female	33	Liposuction	Abdomen	cAT3G5Cs (after decontamination); ATMSCs
17	Female	42	Dermolipectomy	Not assessed	cAT3G5Cs, ATMSCs
18	Female	40	Liposuction	Lower back	cAT3G5Cs, ATMSCs
19	Male	57	Liposuction	Sides of the abdomen	cAT3G5Cs lost owing to contamination after FACS; ATMSCs
20	Female	31	Liposuction	Lower back sides	cAT3G5Cs, ATMSCs

A question mark beside donor 07 denotes that her age was estimated.
ATMSCs, adipose tissue-derived mesenchymal stromal cells; cAT3G5Cs, cultured adipose tissue-derived $3G5^{+}CD31^{-}$ cells; FACS, fluorescence-activated cell sorting.

(DMEM) containing 10% (v/v) FBS (DMEM/10), 1% Fungizone (Life Technologies do Brasil Ltda, São Paulo, Brazil), and 1% penicillin/streptomycin solution. DMEM used in this study was modified to contain 2.2 g of sodium bicarbonate per liter and 2.6 g of sodium HEPES per liter since the amount of CO_2 used in the incubators was 5%. Cells were maintained in an incubator at 37°C with a humidified atmosphere containing 5% CO_2. Three days later, most nonadherent cells were removed along with medium change, and further medium changes were performed twice a week [14].

When cultures were 90% confluent, the medium was removed; the cells were rinsed once with cell detachment basal solution (CMF-HB-HBSS containing 1 mM sodium pyruvate and 0.5 mM EDTA), and then incubated with the same solution for 1 min. This solution was then replaced by cell detachment solution (cell detachment basal solution containing 0.025% trypsin), and cells were incubated at 37°C for 5–10 min. Cell suspensions were removed from the dishes, mixed with an equal volume of RPMI/10, centrifuged, and resuspended in DMEM/10. Cells were seeded at a density of 250,000 viable cells per 100-mm Petri dish (about 3,500 cells/cm^2) in 7 mL of DMEM/10. Subsequent passages were performed in the same way.

At the end of the second passage, ATMSCs were subjected to analyses or were frozen in FBS containing 10% (v/v) of dimethyl sulfoxide. In some occasions, primary cultures were subjected to flow cytometric analyses; in these cases, trypsin concentration used for cell harvesting was 0.25% instead of 0.025%.

Isolation of AT3G5Cs

After enzymatic disaggregation, cells were transferred to 150-mm Petri dishes at a concentration of 2.5×10^7 viable cells in 20 mL RPMI/2 per dish (about 150,000 cells/cm^2). The bottom of the dishes was coated with 5 mL of RPMI/2 right before addition of the cell suspension to minimize spurious cell attachment. The dishes were incubated at 37°C in a humidified atmosphere with 5% CO_2 from 0.5 to 1.5 h to allow the cells to settle down and attach to the plastic.

After incubation, most nonadherent cells and visible clumps were removed by aspiration of the medium. The remaining nonadherent cells were removed by tilting the dishes and rinsing at least twice with 10 mL of CMF-HB-HBSS, dispensing the solution in zigzag at the most elevated end of the dish, and collecting it at the opposite end. Each 150-mm dish received 10 mL of cell detachment solution and was incubated at 37°C for 10 min. Trypsin was inactivated by addition of 5 mL of RPMI/10 per dish. The contents of each dish were combined in 50-mL tubes and centrifuged. At the end of centrifugation, the cell pellets were combined and counted. Cells were then either subjected to antibody staining for fluorescence-activated cell sorting (FACS) right away or resuspended in 20 mL of RPMI 1640 containing 20% FBS and 50 U of DNase I and

kept at 4°C overnight to start antibody staining the next morning.

For antibody staining, cells were sequentially stained with an anti-CD31 antibody and the 3G5 antibody. The anti-CD31 antibody used was a mouse IgG1 present in the supernatant of the P2B1 hybridoma (Developmental Studies Hybridoma Bank, Iowa City, IA), which was concentrated by centrifugation using Amicon Ultra-15 centrifugal filter units with a nominal molecular weight limit of 100,000 kDa (Millipore, Billerica, MA). The 3G5 antibody (mouse IgM) used corresponded to the supernatant of the 3G5 hybridoma (catalog # CRL-1814; American Type Culture Collection, Manassas, VA) concentrated in the same way. The amounts of concentrated supernatants used in immunostainings were defined by titration assays.

Immunostaining for FACS was performed at low temperatures (4–8°C) throughout the process. Cells were resuspended in cold phenol red-free DMEM containing 2% (v/v) FBS (PRF-DMEM/2) at a concentration of 1×10^8 cells/mL. The P2B1 supernatant concentrate was added to the cell suspension at a concentration of 0.5 μL per 1×10^6 cells. Cells were incubated at 4°C for 30 min and washed by addition of 3 mL of cold PRF-DMEM/2, followed by centrifugation at 400 *g* for 5 min at 8°C. The supernatant was discarded, and cells were resuspended in cold PRF-DMEM/2 at a concentration of 1×10^8 cells/mL. An $F(ab')_2$ fragment of goat anti-murine IgG antibody conjugated with Alexa Fluor 633 (Life Technologies do Brasil Ltda, São Paulo, SP, Brazil) was added to the cell suspension at a concentration of 0.5 μg per 1×10^6 cells. Cells were incubated at 4°C for 30 min and washed by addition of 3 mL of cold PRF-DMEM/2, followed by centrifugation at 400 *g* for 5 min at 8°C. The supernatant was discarded, and cells were washed one additional time. After discarding the supernatant, cells were resuspended in cold PRF-DMEM/2 at a concentration of 1×10^8 cells/mL.

The 3G5 supernatant concentrate was added to the cell suspension at a concentration of 0.5 μL per 1×10^6 cells. Cells were incubated at 4°C for 30 min and washed by addition of cold 3 mL PRF-DMEM/2, followed by centrifugation at 400 *g* for 5 min at 8°C. The supernatant was discarded, and cells were resuspended in cold PRF-DMEM/2 at a concentration of 1×10^8 cells/mL. A goat anti-murine IgM antibody conjugated with Alexa Fluor 350 (Life Technologies) was added to the cell suspension at a concentration of 0.5 μg per 1×10^6 cells. Cells were incubated at 4°C for 30 min and washed by addition of cold 3 mL PRF-DMEM/2, followed by centrifugation at 400 *g* for 5 min at 8°C. The supernatant was discarded, and the cells were resuspended in cold PRF-DMEM/2 at a concentration of 1×10^7 cells/mL. At this point, the cell suspension received the additional 50 U of DNase I per mL to minimize cell clumping and 0.75 μg of 7-aminoactinomycin D (7-AAD; BD Biosciences, San Jose, CA) per mL to identify nonviable (7-AAD^+) cells. A control tube containing 200,000 cells was prepared in the same way as described for the cells immunostained for FACS, except that isotype-matched unspecific antibodies used at a concentration of 1 μg/1×10^6 cells were substituted for the anti-CD31 and the 3G5 antibodies.

FACS was performed using the FACSAria cell sorter equipped with 350 nm, 488 nm, and 647 nm lasers, and a 100-μm-wide nozzle (BD Biosciences). The temperature of the sample compartment was set to 4°C and the sample holder was programmed to spin the sample intermittently. The control tube was run through the sorter to set baseline fluorescence values for each channel used, make any necessary compensation adjustments, and adjust the drop delay parameter. The cell suspension that contained the cells immunostained for sorting was filtered through a 40-μm cell strainer to remove any major clumps, and then run through the sorter. Sorting gates were drawn to allow discrimination of $7\text{-AAD}^-3G5^+CD31^-$ events, $7\text{-AAD}^-3G5^-CD31^+$ events, and $7\text{-AAD}^-3G5^+CD31^+$ events. The sorting mask was set to purity or single cell.

Sorted cells were collected either in 15-mL conical tubes containing 6 mL of culture medium or directly in six-well culture plates containing 2 mL of culture medium. In the latter case, the number of cells plated per well varied from as few as 5,000 cells to as many as 100,000 cells.

Expansion of AT3G5Cs in culture

During FACS, $3G5^+/CD31^-$ cells were collected directly in six-well plates coated with poly-L-lysine (2 μg/cm^2) and containing 2 mL of PM. PM consisted of a proprietary basal medium containing 2% FBS, penicillin/streptomycin solution, and PC growth supplement. The PC growth supplement components and their final concentrations in PM were as follows: bovine serum albumin (BSA; 10 μg/mL), apo-transferrin (10 μg/mL), insulin (5 μg/mL), epidermal growth factor (2 ng/mL), fibroblast growth factor 2 (2 ng/mL), insulin-like growth factor 1 (2 ng/mL), and hydrocortisone (1 μg/mL).

Cells were subcultured whenever they reached 90% confluence. Subculturing was performed as follows: cells were harvested by rinsing the cell monolayers with CMF-HB-HBSS and incubating them with cell detachment solution at 37°C for 5 min; the resulting cell suspensions were mixed with one volume of RPMI/10 for every four volumes of cell suspension and centrifuged; the cells were resuspended in PM, counted, and seeded in new poly-L-lysine-coated flasks at a density of 1,000 cells/cm^2.

Flow cytometry

For direct detection of surface molecules by flow cytometry, 1×10^5 cells were resuspended in 100 μL of PBS or culture medium containing 2% FBS and were stained with 0.1 μg of fluorochrome-labeled antibody for 20 min at room temperature in the dark. Antibodies used included anti- CD13, CD14, CD29, CD31, CD34, CD44, CD45, CD49a, CD49e, CD51/61, CD54, CD56, CD73, CD90, CD105, CD106, CD144, CD140b, CD146, CD166, CD271, KDR, HLA-ABC, and HLA-DR or isotype controls (BD Biosciences). After washing with PBS, cells were resuspended into 300 μL of PBS, and fluorescence was read in a FACSCalibur flow cytometer (BD Biosciences).

The anti-nerve/glial antigen 2 (NG2) antibody used was from R&D Systems (Minneapolis, MN). The 3G5 antibody was used in line with an Alexa Fluor 488-conjugated anti-IgM secondary antibody (Life Technologies). In some occasions, fluorescence was read in a FACSAria cell sorter. In some experiments, cells received concomitant addition of two antibodies labeled with nonoverlapping fluorochromes. Flow cytometry histograms were generated using Cyflogic 1.2.1 (CyFlo Ltd, Turku, Finland; freely available at http://www.cyflogic.com/).

For a detailed comparison of frequencies of positive cells and geometric mean fluorescence intensity (MFI), four ATMSC and four cAT3G5C populations from matching donors (ATMSCs 06, 08, 09, and 10, and cAT3G5Cs 06, 08, 09, and 10), which were established after the implementation of the adherence selection step, were harvested at the end of the second or third passages. Frequencies of positive cells were obtained by subtracting the frequency of false-positive events in control tubes from the frequency of positive cells in tubes stained for the indicated surface molecules.

Sample size for most analyses was four in each group (ATMSCs or cAT3G5Cs), with rare exceptions in some cases, in which data were missing owing to faulty or missing antibodies used on the days of the data acquisitions. These exceptions were CD49e and CD56 in cAT3G5Cs 09, CD166 in ATMSCs 10, and NG2 in ATMSCs 08, ATMSCs 09, cAT3G5Cs 08, and cAT3G5Cs 09. Student's *t*-test was used for statistical comparisons of frequencies or log(2) MFIs of each marker between ATMSCs and cAT3G5Cs, except when data did not pass tests for normality or homogeneity of variance. In these cases, Mann–Whitney rank sum tests were used to detect significant differences. Differences were considered significant when the calculated P value was ≤ 0.01.

Differentiation assays

Osteogenic differentiation was performed on ATMSCs or cAT3G5Cs from matching donors at similar passage numbers. Cells used in the experiments were harvested between passages 3–7. Cells were seeded at a density of 5×10^4 cells per well in six-well dishes in 2.5 mL of DMEM/10 containing 1×10^{-8} M dexamethasone and 50 μg/mL ascorbic acid 2-phosphate for 10 days when this medium formulation was augmented with 2 mM β-glycerophosphate and cells were cultured for additional two weeks. Calcium-rich extracellular matrix (ECM) was detected by staining with Alizarin Red S.

Adipogenic differentiation was performed on ATMSCs or cAT3G5Cs from matching donors at similar passage numbers. Cells used in the experiments were harvested between passages 3–7. Cells were seeded at a density of 1×10^5 cells per well in six-well dishes in DMEM/10 containing 1×10^{-8} M dexamethasone and 5 μM rosiglitazone for 7 to 10 days when this medium was augmented with 5 μg/mL bovine insulin and cells were cultured for additional time (1–2 weeks). Lipid-containing vacuoles were stained with Oil Red O, and cells were counterstained with Harris hematoxylin.

For chondrogenic differentiation, cells were harvested between passages 3–7, washed in serum-free DMEM, and resuspended at a concentration of 1×10^6 cells/mL in a defined chondrogenic medium (high-glucose DMEM, 1% ITS+, 1% nonessential amino acids, 1 mM sodium pyruvate, 1×10^{-7} M dexamethasone, 50 μg/mL ascorbic acid 2-phosphate, and 100 ng/mL transforming growth factor β3 [15,16]). Cells were dispensed into polypropylene freezing vials with a conical bottom at a density of 250,000 cells per tube and placed in a tissue culture incubator with the cap slightly loose to permit gas exchange. Cells deposited to the bottom of the tubes and formed aggregates, which were cultured for 3 weeks in 250 μL of chondrogenic medium with three medium changes a week. At the end of the culture period, cell aggregates were washed in PBS, fixed for 15 min in 4% paraformaldehyde in PBS, washed once again with PBS, and subjected for standard processing for paraffin embedding. Cell aggregates were sectioned at 5 μm, transferred to histological slides, deparaffinized, and stained with Toluidine Blue O to allow visualization of sulfated glycosaminoglycans by metachromasia (color change from blue to purple).

Inhibition of T-cell proliferation assay

The inhibitory effect of PCs and ATMSCs from two different donors on allogeneic lymphocyte proliferation was tested using the carboxyfluorescein diacetate succinimidyl ester (CFSE) dilution method as follows. Peripheral blood mononuclear cells (PBMNCs) from healthy donors were isolated by centrifugation of peripheral blood samples on a Ficoll-Hypaque density gradient, labeled with CFSE (Life Technologies) at a final concentration of 10 μM for 10 min at 37°C, and resuspended in RPMI supplemented with 5% human serum albumin.

CFSE-labeled PBMNCs (5×10^5 cells/mL) were added to 24-well plates (1 mL/well), which had been previously seeded with PCs or ATMSCs at six different PC:PBMNC or ATMSC:PBMNC ratios (1:2, 1:5, 1:10, 1:20, 1:50, and 1:100) in the presence of 0.5 μg/mL of phytohemagglutinin. Cocultures were incubated for 5 days at 37°C in an atmosphere containing 5% CO_2. On the fifth day of coculture, PBMNCs were harvested, stained with a phycoerythrin-conjugated anti-CD3 antibody (BD Biosciences), and analyzed by flow cytometry to determine the intensity of CFSE fluorescence in $CD3^+$ cells. Controls included CFSE-labeled PBMCs stimulated with phytohemagglutinin in the absence of PCs or ATMSCs and CFSE-labeled PBMNCs cultured in the absence of phytohemagglutinin, PCs, or ATMSCs.

Karyotyping

PCs used for cytogenetic investigation were harvested at the third passage and treated with colcemid solution (Irvine Scientific, Santa Ana, CA) at 37°C for 1 h. Cells were subjected to hypotonic treatment by incubation in KCl solution at 37°C for 20 min and fixed with methanol and acetic acid according to standard procedures. Metaphases were G-banded with trypsin (Irvine Scientific).

Criteria for defining an abnormal karyotype were the presence of at least two metaphases showing the same structural abnormality or chromosome gain in at least two metaphases or loss of the same chromosome in at least three metaphase cells. The metaphase images were acquired using an Axio Imager M2 microscope (Zeiss, Jena, Germany) equipped with BandView software, version 5.5 (ASI, Carlsbad, CA). Automatic identification of chromosomes was based on the average resolution of 450 bands per haploid set. A minimum of 20 metaphases were analyzed using the BandView software (ASI).

Slides for spectral karyotype (SKY) analysis were prepared using the same fixed chromosome preparations employed for G-banding analysis. Chromosome labeling was done with an SKY fluorescent labeling kit (Applied Spectral Imaging, Migdal HaEmek, Israel) according to the manufacturer's protocol. Image acquisition was performed with an SD200 Spectracube (Applied Spectral Imaging)

mounted on an Axio Imager M2 microscope (Zeiss) using a custom-designed optical filter (SKY-1; Chroma Technology, Brattleboro, VT). Automatic identification of chromosomes was based on the measurement of the spectrum for each chromosome. A minimum of 20 metaphases were analyzed using the SkyView 5.5 software (ASI).

Immunofluorescence

Subcutaneous AT fragments of around 2 cm^3 from patients who underwent dermolipectomy surgeries were included in optimal cutting temperature compound (OCT) and frozen in liquid nitrogen. Specimens were sectioned in a cryostat at a temperature of −20°C; section thickness was set to 7 μm. Sections were transferred to gelatin-coated glass slides and stored at −20°C until use.

All procedures used for immunostaining were performed at room temperature. Slides used for immunostaining were rinsed with PBS to remove OCT, and sections were circled with a histological pen. Before antibody staining, slides were incubated with 5% nonfat powdered milk in PBS for 30 min to minimize nonspecific antibody binding. Sections were then covered with the supernatant of the 3G5 hybridoma and incubated for 30 min. After rinsing with 0.5% nonfat milk in PBS, sections were incubated for 30 min with an Alexa Fluor 488-conjugated goat anti-mouse IgM antibody (Life Technologies) at a concentration of 0.5 μg/mL in PBS containing 1% BSA. Sections were rinsed with 0.5% nonfat milk in PBS, covered with the supernatant of the P2B1 hybridoma, and incubated for 30 min. Sections were rinsed with 0.5% nonfat milk in PBS, and then incubated with an Alexa Fluor 594-conjugated goat anti-mouse IgG at a concentration of 0.5 μg/mL in PBS containing 1% BSA for 30 min.

Slides were rinsed with PBS and incubated with a 4′,6-diamidino-2-phenylindole (DAPI) solution for 15 min before mounting with a coverslip. Mounting medium consisted of a 1:9 mixture of PBS and glycerol containing a final concentration of 5 mg/mL of n-propyl gallate. Control slides were prepared in the same way as described above, except that nonspecific isotype-matched antibodies at a concentration of 0.5 μg/mL were substituted for the 3G5 and P2B1 antibodies. Slides were analyzed under an upright epifluorescence microscope (Axioskop2; Zeiss) or on an inverted confocal microscope (LSM 710; Zeiss). Images were captured through digital cameras attached to the microscopes using the software provided by the manufacturer.

Microarray hybridization and scanning

RNA was extracted using TRIzol LS reagent (Life Sciences) and cleaned up using the RNeasy mini kit (QIAGEN Biotecnologia Brasil Ltda, São Paulo, Brazil) following manufacturers' instructions. RNA was quantified using a NanoDrop 1000 spectrophotometer (ThermoScientific, Wilmington, DE).

Oligonucleotide microarrays from two 4×44K Whole Human Genome Microarray Kits (Agilent, G4112F, and G4845A; design IDs 014850 and 026652, respectively), which contain probes for more than 41,000 gene transcripts, were used to analyze gene expression of the samples. A predetermined amount of control bacterial RNA from the One-Color RNA Spike-In Kit (5188-5282; Agilent) was added to total RNA before synthesis of complementary RNA (cRNA) and labeling with cyanine 3 (Cy3) using the One-Color Quick Amp Labeling Kit (5190-0442; Agilent). RNA was reverse transcribed using oligo (dT) containing a promoter for RNA T7 polymerase. The resultant cDNA was purified, fragmented, and used as template for cRNA in vitro transcription using T7 RNA polymerase and nucleotides, which included Cy3-CTP for labeling. The cDNA obtained was purified using the Illustra RNAspin mini Kit (25050071; GE Life Sciences).

cDNA quantitation and labeling efficiency were determined using a NanoDrop 1000 spectrophotometer (ThermoScientific). Labeled cRNA was hybridized with microarray slides using the Gene Expression Hybridization Kit (5188-5242; Agilent) in SureHyb hybridization chambers (G2534A; Agilent) for 17 h at 65°C at 10 RPM in a hybridization oven (G2545A; Agilent). After hybridization, microarray slides were washed and dried. The slides were then scanned at 535 nm with a resolution of 5 μm/pixel using a DNA Microarray Scanner with Sure Scan High-Resolution Technology (Agilent Technologies). Expression data were extracted using Agilent's Feature Extraction software versions 8.5 or 11.5. Microarray raw data files have been deposited in NCBI's Gene Expression Omnibus (GEO; www.ncbi.nlm.nih.gov/geo/) as data series GSE67747.

Microarray analyses

To compare data from the two microarray design IDs, one tab-delimited text file corresponding to each design was selected to define probes common to both using Microsoft Excel's VLOOKUP function after filtering out probes corresponding to controls. Since both designs contain a nonmatching number of repeated probes, the resulting probe list had duplicate probes removed by checking the option, unique records only, in Excel's advanced filter. The resulting unique probe list, which contained 18,561 probes, was used as a reference to remove probes (and their associated parameter values), which were not shared by both designs using Excel's VLOOKUP function after organizing probe names in the ascending order. Nonunique probes were removed using Excel's advanced filter, and data files were used for downstream analyses.

Analyses were performed using BRB-ArrayTools (version 4.3.1) developed by Dr. Richard Simon and the BRB-ArrayTools Development Team, available at http://linus.nci.nih.gov/BRB-ArrayTools.html. Data files were imported to BRB-ArrayTools using its general format importer tool. The unique ID was defined as the probe name, the intensity value was set as the processed signal of the green channel (gProcessedSignal column), the column, gIsFeatNonUnifOL, was set as a flag, and the column, gNumPix, was set as the spot size descriptor. Expression data were converted to log2 values and subjected to quantile normalization. Whenever samples were grouped, log2 expression values for each probe were averaged within each group.

Statistical analyses were performed using the class comparison between groups of arrays tool in BRB-ArrayTools using default settings, which include a nominal significance level of 0.001 for each univariate test. Before these analyses, samples were grouped according to their characteristics, flagged spots and spots with a size <10 were removed, and

genes that contained more than 50% of missing values were excluded.

To detect pathways over-represented in gene lists resultant from statistical analyses, gene lists were analyzed using the Functional Annotation Tool in Database for Annotation, Visualization and Integrated Discovery (DAVID) v6.7 at http://david.abcc.ncifcrf.gov/home.jsp. The identifiers used in these gene lists were the probe names, which correspond to AGILENT_ID in DAVID. The background used was *Homo sapiens*. Kyoto Encyclopedia of Genes and Genomes (KEGG) pathways were selected for analysis. Pathways with a Benjamini–Hochberg-corrected P value ≤ 0.05 were considered significantly enriched in the gene lists analyzed.

For clustering experiments, expression intensity values were thresholded to eight to reduce background noise; subsequently, samples were clustered using the Euclidean distance with average linkage. Data files included in the clustering experiments were either generated in this study or obtained from GEO.

Data generated by us included ATMSCs 16–18 (harvested at the end of passage 2), ATMSCs from donor 18 cultured in PM (ATMSCs 18 PM; harvested at the end of passage 5), cultured adipose AT $3G5^+/CD31^-$ cells cultured in PM (cAT3G5Cs) 1–3 [harvested at the end of passages 6 (cAT3G5Cs 1 and 2) and 7 (cAT3G5Cs 3)], and cAT3G5Cs 1–3 cultured in DMEM + 10% FBS (cAT3G5Cs 1–3 DME10; harvested at the end of the second passage), GEO accessions GSM1655122-GSM1655131, respectively.

Data obtained from GEO were as follows: bone marrow MSCs (BMMSCs) 1–5, GEO accessions GSM451463, GSM451464, GSM451465, GSM451466, and GSM451467, respectively [17]; dermal fibroblasts (dermal FBs), GEO accession GSM242095, induced pluripotent stem cells derived from dermal fibroblasts (dermal FB iPSCs), GEO accession GSM241846 [18]; airway fibroblasts (airway FBs) 1–3, GEO accessions GSM385592, GSM385593, and GSM385594, respectively; distal lung fibroblasts (distal lung FBs) 1–3, GSM385595, GSM385596, and GSM385597, respectively [19]; human microvascular endothelial cells, GEO accession GSM1103367 [20]; human umbilical vein endothelial cells (HUVECs) 1–3, GEO accessions GSM418611, GSM418615, and GSM418619, respectively [21]; HUVECs (senescent), GEO accession GSM910552, HUVECs (young), GEO accession GSM910550 [22]; human embryonic stem cells (hESCs) H9, BG03, and ES01, GEO accessions GSM910550, GSM194390, and GSM194391, respectively [23]; peripheral blood white blood cells (PBWBCs) 1–5, GEO accessions GSM469524, GSM469528, GSM469532, GSM469536, and GSM469540, respectively [24]; and dental pulp stem cells (DPSCs) 1–3, GEO accessions GSM1105733, GSM1105734, and GSM1105735, respectively [25].

Results

Isolation and culture of AT3G5Cs

The frequency of $3G5^+$ cells was highly variable in SVF cells analyzed right after enzymatic disaggregation: 1%, 1%, 3%, 9%, 10%, and 21% in samples from six different tissue donors. Even though cells that expressed the 3G5 antibody-defined antigen at high levels could be clearly detected in these samples, it was likely that a number of cells that expressed this antigen at lower levels were not detectable because of the high background fluorescence levels owing to dead cells and debris resultant from the enzymatic disaggregation procedure. The number of $3G5^+$ cells was variable also in primary ATMSC cultures: 9%, 14%, 27%, and 36% in primary cultures from four different tissue donors.

While seeking for an explanation for the highly variable apparent frequency of $3G5^+$ cells in the SVF, we checked the material retained in cell strainers used to remove gross remnants of one freshly disaggregated tissue sample and found that those remnants comprised mainly integer blood vessels of small caliber. Observation of this material under phase contrast indicated that many PCs remained attached to these vessels (not shown). This finding called for an increase in collagenase concentration, which was detrimental to cell viability. To circumvent that problem, we performed enzymatic disaggregation in medium containing 2% FBS; this would prevent tryptic activity, but preserve collagenolytic activity.

After processing one AT sample in this way, the resulting population was immunostained to allow detection of $3G5^+CD31^-$ cells, which were selected by FACS, and cultured in standard MSC medium. However, even after a week in culture, the adherent cells did not proliferate. When the medium was switched to a formulation optimized for human PC expansion, these cells became proliferative and gave rise to the first cAT3G5C population. From then on, AT3G5Cs isolated by FACS were directly cultured under PC conditions. This isolation and expansion procedure was successfully applied to samples from other tissue donors (Table 1); however, in some instances, variable numbers of cells that failed to adhere were present in primary cultures in spite of previously coating the plates with poly-L-lysine (not shown). Additionally, the high fluorescent noise caused by dead cells and debris during AT3G5C detection for FACS persisted.

Since the adherent fraction of primary adipose stromal cultures contained $3G5^+$ cells, we hypothesized that adherence to plastic could be used both as a functional criterion for the selection of $3G5^+$ cells and as a way to remove most debris from the samples. Therefore, stromal–vascular cells obtained after enzymatic disaggregation of AT were dispensed into culture-treated plastic dishes in culture medium containing a minimal amount of FBS (2%) and allowed to attach for only a minimal amount of time (0.5 to 1.5 h) to minimize phenotypical changes before immunostaining for FACS. Removal of nonadherent cells and debris by washing with saline solution, followed by harvesting of the cells with a low trypsin concentration, yielded a cell sample with high quality for FACS.

In one experiment designed to visually assess the efficacy of the isolation methodology, cells isolated by FACS were inspected 12 h after plating; the vast majority of the $3G5^+CD31^-$ cells were found well attached to the bottom of the plates, while most of the $3G5^-CD31^+$ cells failed to adhere and spread on the substratum (Fig. 1). cAT3G5Cs exhibited cell projections up to the third day in culture (Fig. 2A) and became fibroblastoid thereafter (Fig. 2B–D). Average population duplication time was 1.5 day during the first three passages (not shown). Three cAT3G5C populations were checked for chromosomal abnormalities using classical G-band karyotyping and spectral karyotyping, with no cytogenetic alterations detected (Fig. 2C).

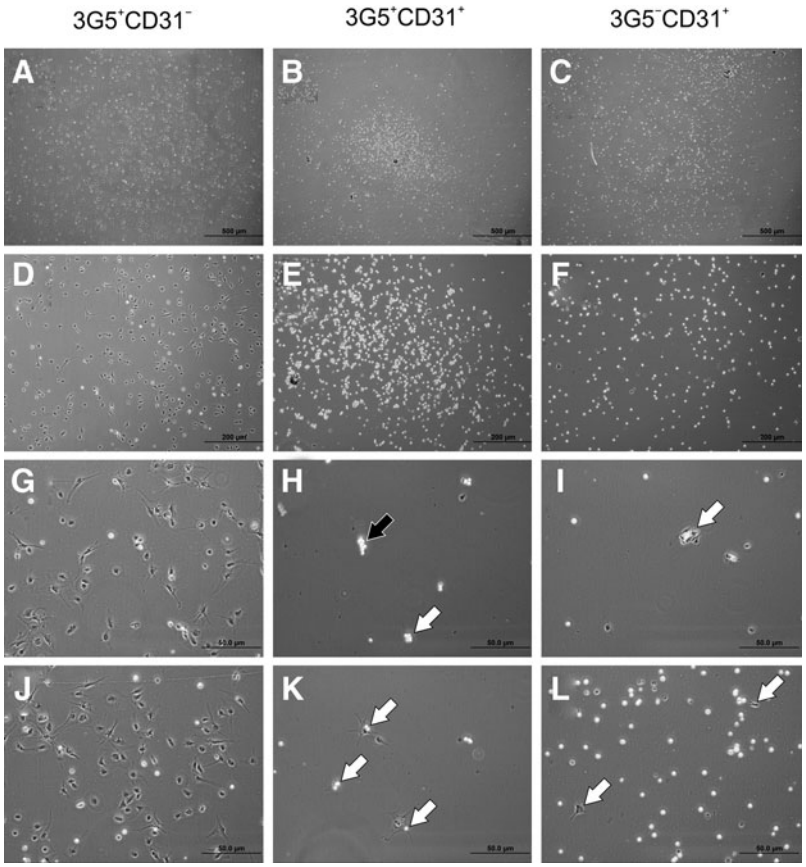

FIG. 1. Morphology of $3G5^{+}CD31^{-}$ cells, $3G5^{+}CD31^{+}$ cells, and $3G5^{-}CD31^{+}$ cells after 12 h in culture. **(A–F)** Low-power images demonstrate cells derived from $3G5^{+}CD31^{-}$ cells **(A, D)**, which were adherent in their majority compared with cells derived from $3G5^{+}CD31^{+}$ cells **(B, E)**, or $3G5^{-}CD31^{+}$ cells **(C, F)**, which were nonadherent in their majority. **(G–L)** Higher power images that detail the morphology of the adherent cells derived from the three cell populations examined. **(H, K)** Adherent cells with a pericytic morphology aggregated with nonadherent cells are visible (*white arrows*). **(H)** A cell clump corresponding to a microvessel fragment is indicated by a *black arrow*. **(I)** Adherent cells with endothelial morphology are indicated (*white arrow*). **(L)** *White arrows* indicate adherent cells with a cell morphology characteristic of macrophages.

In vitro functional characterization of cAT3G5Cs and ATMSCs

When cultured under adipogenic conditions, the frequency of adipocytes originating from cAT3G5Cs was far superior compared with MSCs cultured under the same conditions (Fig. 3A, E, I, J). In some experiments, the frequency of lipid vacuole-rich cells in cAT3G5Cs subjected to adipogenic conditions was visually estimated to be above 95%. cAT3G5Cs also deposited more mineralized matrix than MSCs (Fig. 3C, G, L, M). To verify that cAT3G5Cs meet minimal differentiation criteria to be classified as MSCs, we also subjected them to chondrogenic culture conditions. Staining of histological sections of chondrogenic pellets showed that cAT3G5Cs produced sulfated glycosaminoglycans as detected by Toluidine Blue metachromasia (Fig. 3O).

During the differentiation experiments of one of the cAT3G5C populations established without the adherence selection step, we could observe the formation of multinucleated tubes, some of which are able to contract (Fig. 3P). In that case, the myogenic cells were considered to be derived from muscle tissue scraped off during the liposuction procedure as $\sim$2% of these cAT3G5Cs expressed CD56 (Fig. 3Q), a marker present in myogenic muscle cells [26]. In agreement with this, myogenic cells were not observed in any of the $3G5^{+}CD31^{-}$ cell populations established from subcutaneous fat obtained from patients who underwent postbariatric dermolipectomy surgeries. Interestingly, we did not observe myotube formation in any of the cAT3G5Cs established after using the adherence selection step. In one experiment, a culture established by $3G5^{+}CD31^{-}$ cells isolated by FACS after adherent cell selection was compared with a culture established by $3G5^{+}CD31^{-}$ cells from the same donor that were not subjected to this procedure. Flow cytometry analyses indicated that both cell populations were similar, except that cAT3G5Cs established without the adherence step contained a small number of $CD56^{+}$ cells (not shown). Therefore, the adherence selection step seemed to eliminate $CD56^{+}$ cells derived from muscle that were scraped off during liposuction surgeries and could give rise to myotubes in culture.

Finally, both cAT3G5Cs and ATMSCs were able to inhibit $CD3^{+}$ cell proliferation induced by phytohemagglutinin when cocultured with PBMNCs for 5 days (Fig. 3R). Performance of both cell populations was similar, with inhibition of $CD3^{+}$ cell proliferation becoming apparent at a proportion of one cell to 20 PBMNCs. A nearly complete inhibition of $CD3^{+}$ cell proliferation was attained at a proportion of one cell to five PBMNCs. No statistical differences between cAT3G5Cs and ATMSCs within each cell:PBMNC proportion were found using Student's *t*-test.

cAT3G5Cs and ATMSCs display a congruent immunophenotype

When cAT3G5Cs were analyzed by flow cytometry, they were found to exhibit a surface molecule profile essentially identical to that of ATMSCs from the same donors (Fig. 4A–D). We applied statistical tests to determine if differences between ATMSCs and cAT3G5Cs were detectable. We observed that a difference in frequency of $CD13^{+}$ cells

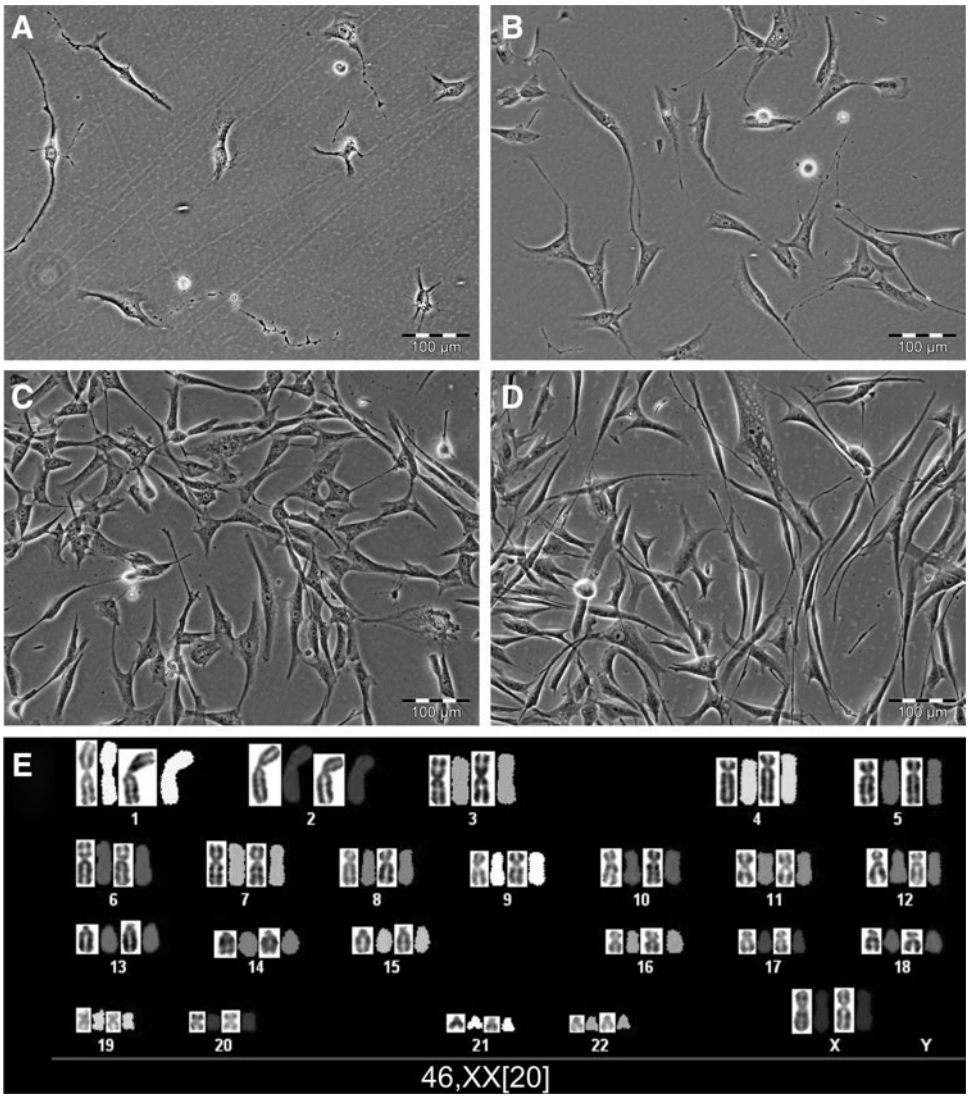

FIG. 2. Morphology and cytogenetics of cAT3G5Cs. **(A)** On day three after isolation, cAT3G5Cs exhibited various morphologies, with a few or multiple cellular projections. **(B)** On day 5 after isolation, cAT3G5Cs were already fibrolastoid. This morphology was maintained on day 7 after isolation **(C)** and after serial passaging. **(D)** cAT3G5Cs after the first passage. **(E)** Spectral karyotype of cAT3G5Cs. cAT3G5Cs, cultured adipose tissue-derived $3G5^{+}CD31^{-}$ cells.

between these populations was statistically significant at $P \leq 0.05$ ($P = 0.0308$), but such a difference did not make sense in a biological context as both cell populations exhibited nearly 99% of positive cells (averages were 98.975 in ATMSCs and 99.5475 in cAT3G5Cs). Therefore, we decided to consider differences statistically significant at $P \leq 0.01$. Consequently, no statistical differences were detected between ATMSCs and cAT3G5Cs regarding frequency of positive cells or geometric MFI for each surface molecule analyzed.

While the frequency of cells positive for surface markers typically associated with MSCs, such as CD13, CD29, CD44, CD73, CD90, CD105, and CD166, was invariable, the frequency of $CD146^{+}$ cells was variable in cAT3G5Cs and ATMSCs. Since we found that CD146 was not subjected to variation in BMMSCs routinely analyzed using the same antibody in the same flow cytometry facility, and which were harvested using a trypsin concentration 10 times higher than that used in this study (0.25% vs. 0.025%, respectively; not shown), the possibilities that the anti-CD146 antibody used was faulty and that CD146 is sensitive to trypsin were excluded. Since CD146 has been reported to be subject to cleavage by matrix metalloproteinase 3 (MMP3) [27], we decided to check expression of this enzyme in the microarray data used in this study. Consequently, we found that cAT3G5Cs and ATMSCs express this enzyme, while BMMSCs do not (Fig. 4E). Therefore, variability on CD146 expression on the surface of cAT3G5Cs and ATMSCs may be explained by cleavage of CD146 by autogenous MMP3.

In addition to the molecules above, both cAT3G5Cs and ATMSCs did not express EC markers, such as CD31 or KDR, nor did they exhibit the hematopoietic markers, CD45 and CD14. Both cell populations were positive for the PC markers, CD140b and NG2, and were negative for CD34, CD56, CD106, CD271, and HLA-DR. CD49a, CD49e, CD51/61, CD54, and HLA-ABC were also expressed by cAT3G5Cs and ATMSCs. The frequency of $3G5^{+}$ cells in both populations was minimal, which indicates that expression of the 3G5-defined antigen was lost in culture. Since cAT3G5Cs expressed the activated PC marker, NG2 (a.k.a. high-molecular-weight melanoma-associated antigen) [28], loss of expression of the 3G5 antigen by these cells in culture is likely to reflect transition from a resting PC phenotype (AT3G5Cs) to an activated PC phenotype rather than inability of PM to support maintenance of a pericytic phenotype.

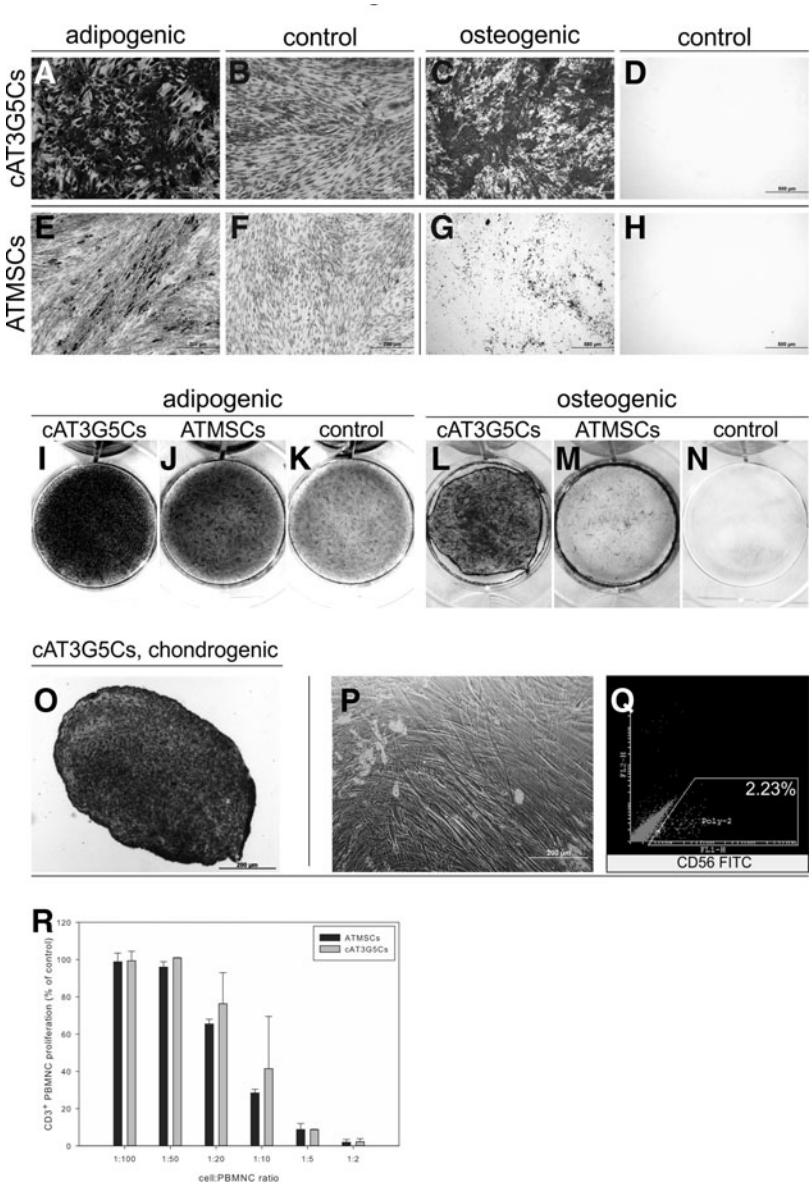

FIG. 3. In vitro functional characterization of cAT3G5Cs and ATMSCs. **(A)** cAT3G5Cs subjected to adipogenic differentiation, stained with Oil Red O to show lipid-laden vacuoles (visible as *dark gray—black* in *grayscale*), and counterstained with Harris hematoxylin. **(B)** Negative control for **(A)**. **(C)** Micrograph of cAT3G5Cs subjected to osteogenic differentiation and stained with Alizarin Red S, which highlights calcium in the extracellular matrix in *red* (visible as *dark gray—black* in *grayscale*). **(D)** Negative control for **C**. **(E)** Micrograph of ATMSCs subjected to adipogenic differentiation, stained with Oil Red O, and counterstained with Harris hematoxylin. **(F)** Negative control for **E**. **(G)** ATMSCs subjected to osteogenic differentiation and stained with Alizarin Red S. **(H)** Negative control for **G**. **(I–N)** Macroscopic views of **A**, **E**, **F**, **C**, **G**, and **H**, respectively. Staining intensity is proportional to the intensity of *black* **(I–N)**. **(O)** Section of a chondrogenic pellet formed by one cAT3G5C population, stained with Toluidine Blue, which changes color from *blue* (which would correspond to a *dark shade of gray* in *grayscale*) to *purple* (shown as a *light shade of gray*) in the presence of sulfated glycosaminoglycans characteristic of cartilage. **(P)** Myotubes formed in a cAT3G5C culture established from liposuction material without the adherence selection step. **(Q)** Flow cytometry dot plot showing the presence of a minor population (around 2%) of $CD56^+$ cells (possibly contaminating myogenic cells scraped off muscle during liposuction) in a cAT3G5C culture established without the adherence step. **(R)** In vitro suppression of $CD3^+$ lymphocyte proliferation by cAT3G5Cs and ATMSCs. ATMSCs, adipose tissue-derived mesenchymal stromal cells.

AT3G5Cs exhibit CD34, CD140b, and CD271 on their surface, but not CD146

When the methodology for AT3G5C isolation was fully developed, the isolated cells were subjected to immunophenotyping right after FACS. Two immunostaining experiments were performed (Fig. 5A, B). The analyses indicated that freshly isolated AT3G5Cs were indeed free from ECs since no $CD144^+$ cells were clearly detectable. Hematopoietic cells, identifiable by CD45 expression, were also not detected. The vast majority of freshly isolated AT3G5Cs were positive for CD140b and for CD34. Interestingly, at least half of these cells were positive for the low affinity nerve growth factor receptor, CD271.

CD146, a marker for endothelial and smooth muscle cells [7], was not detectable on the surface of AT3G5Cs. As mentioned in the previous section, the absence of detection of CD146 on the surface of these cells could not be attributed to a defective anti-CD146 antibody because this reagent did react against CD146 on the surface of BMMSCs routinely analyzed in the same flow cytometry facility. Additionally, cleavage of CD146 owing to tryptic activity of type I collagenase is excluded because tissue disaggregation was performed in the presence of FBS, whose antitrypsin extinguishes tryptic activity present in this enzymatic preparation. It is noteworthy that the absence of CD146 expression has been previously demonstrated in the $CD34^+$ fraction of human AT SFV [29] to which AT3G5Cs belong. Therefore, the absence of surface CD146 is a genuine characteristic of AT3G5Cs.

In the first immunophenotyping experiment performed, cells were also stained with antibodies raised against KDR, CD56, HLA-DR, and NG2. NG2 was barely detectable on the surface of the AT3G5Cs; HLA-DR seemed to be expressed at very low levels on the surface of a subpopulation of <5% of $CD140b^+$ cells; KDR and CD56 were not detected.

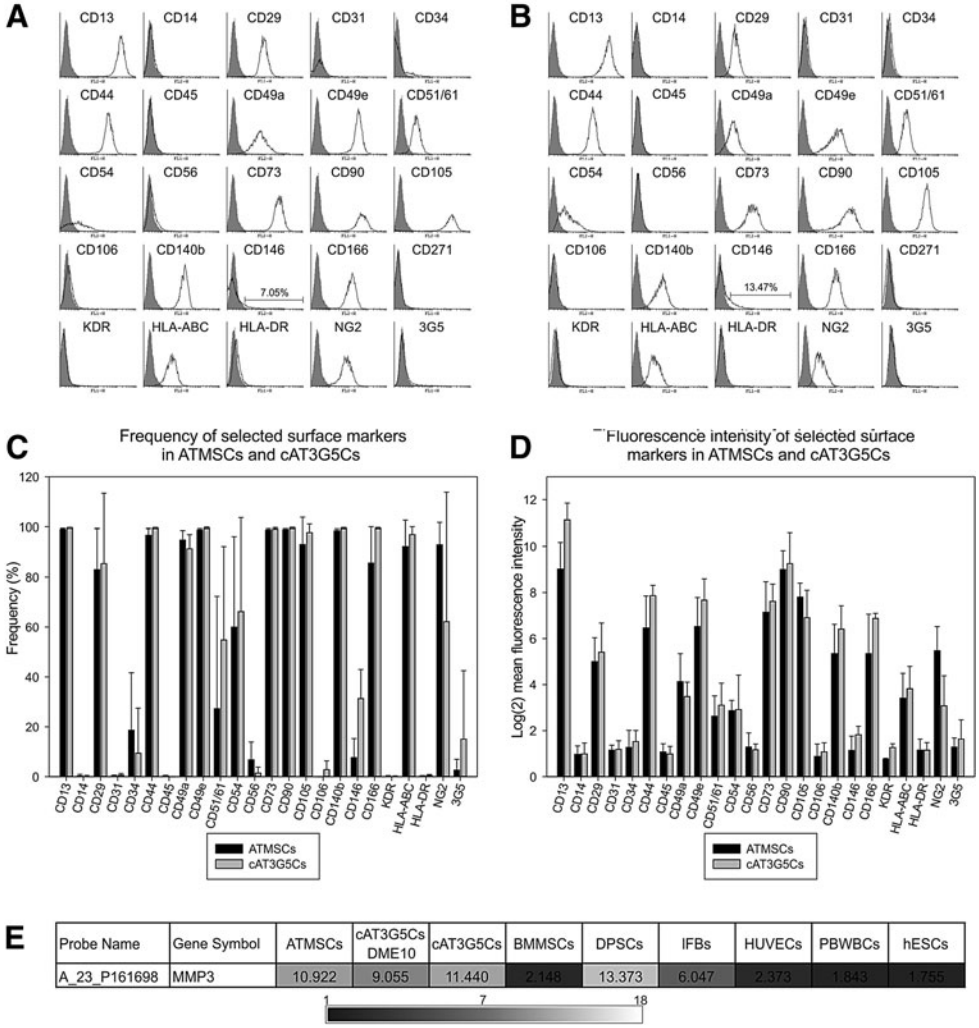

FIG. 4. Immunophenotype of ATMSCs, cAT3G5Cs, and freshly isolated AT3G5Cs. *Solid line* histograms depict the expression of the indicated molecules in ATMSCs **(A)** or cAT3G5Cs **(B)** from the same donor compared with negative controls (*shaded* histograms), representative of at least three immunophenotypings, in which ATMSCs and cAT3G5Cs from different donors were compared with each other. **(C)** Frequencies of cells positive for the indicated surface molecules in ATMSCs and cAT3G5Cs. Bars represent standard deviation. **(D)** Log(2) means fluorescence intensities (MFIs) of the indicated surface molecules in ATMSCs and cAT3G5Cs. Bars represent standard deviation. **(E)** Normalized log(2) expression levels of matrix metalloproteinase 3 (MMP3) by ATMSCs, cAT3G5Cs, cAT3G5Cs cultured in MSC medium (cAT3G5Cs DME10), bone marrow MSCs (BMMSCs), dental pulp stem cells (DPSCs), lung fibroblasts (lFBs), human umbilical vein endothelial cells (HUVECs), peripheral blood white blood cells (PBWBCs), and human embryonic stem cells (hESCs). Table cells were colored to reflect MMP3 gene expression intensity shown in the scale below it.

AT3G5Cs are periendothelial in vivo

As a final step to confirm that the AT3G5Cs isolated by us correspond to PCs, we decided to directly observe the microanatomical location of $3G5^+$ cells in human AT. Analyses of 7-μm-thick cryosections from subcutaneous AT revealed the presence of $3G5^+$ cells physically associated with $CD31^+$ capillaries in a periendothelial manner (Fig. 6). Confocal laser microscopy confirmed that expression of the antigen defined by the 3G5 antibody and CD31 did not colocalize (Fig. 6C–F). We failed to detect a signal from the 3G5 antibody in cell types outside the vasculature. We verified the absence of unspecific immunostaining in negative controls.

The gene expression profile of cAT3G5Cs is very similar to that of ATMSCs

When three populations of cAT3G5Cs and three populations of ATMSCs were included in clustering analyses along with other cell types, ATMSCs were found to cluster closer to other adult MSCs (BMSCs, DPSCs) or fibroblasts rather than remaining close to cAT3G5Cs (Fig. 7). We hypothesized that these results reflected the effect of different culture conditions on cAT3G5Cs and ATMSCs. Therefore, we cultured the same three cAT3G5Cs under ATMSC conditions for two passages and used their RNAs to prepare new microarrays. When these data were included in the clustering analyses, cAT3G5Cs cultured under ATMSC

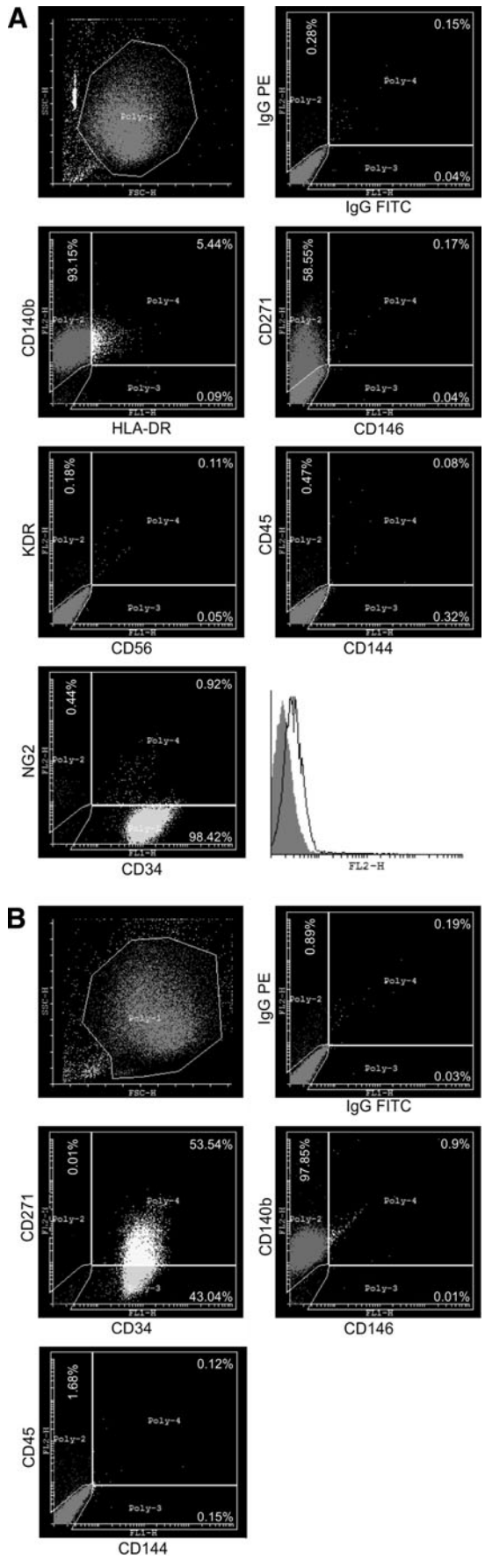

conditions (cAT3G5Cs DME10) not only clustered close to ATMSCs but also merged in a single cluster with them (Fig. 7). We next asked if an ATMSC population would acquire the characteristics of cAT3G5Cs when cultured in PM. When microarray data from one ATMSC population subjected to culture in PM (ATMSCs 18 PM) were included in a clustering analysis, this population clustered with cAT3G5Cs (Fig. 7), which reinforces the similarity between ATMSCs and cAT3G5Cs.

To further investigate the seemingly minor differences between cAT3G5Cs DME10 ($n=3$) and ATMSCs ($n=3$), their microarray data were statistically compared using a nominal significance level of 0.001. The expression levels, only 222 transcripts (1.2% of a total of 18,561 transcripts), were found to be significantly different between these two cell populations (Table 2). This is in contrast with the number of transcripts whose levels were significantly different when cAT3G5Cs 1–3 and cAT3G5Cs 1–3 DME10 were compared with each other (2,003 transcripts, or 10.8% of the total number of transcripts), or when cAT3G5Cs 1–3 and ATMSCs 16–18 were compared with each other (2,481 transcripts, or 13.4% or the total number of transcripts).

When we focused on the transcripts differentially expressed when cAT3G5Cs DME10 and ATMSCs were compared with each other, we found that 75 (0.4%) were upregulated in cAT3G5Cs DME10 compared with ATMSCs and 147 (0.8%) were upregulated in ATMSCs compared with cAT3G5Cs DME10 (Table 2). Seven of the transcripts upregulated in ATMSCs corresponded to EC markers (*LIPG*, *PECAM1*, *CD93*, *VWF*, *TIE1*, *ECSM2*, and *KDR*), which indicates that at least some of the differences found between cAT3G5Cs DME10 and ATMSCs are attributable to the presence of ECs in the latter, even though endothelial contamination in ATMSC cultures was not detectable by flow cytometry.

No significant pathways emerged when the upregulated transcript lists shown in Table 2 were subjected to an analysis of over-represented signaling pathway components (Table 3), which could be attributed to the very high similarity between cAT3G5Cs DME10 and ATMSCs. In contrast, when genes upregulated in cAT3G5Cs compared with cAT3G5Cs DME10 or ATMSCs were mined, the significant pathways that emerged were essentially associated with cell proliferation and DNA synthesis/repair (Table 3) as cAT3G5Cs were highly proliferative compared with cAT3G5Cs DME10 and ATMSCs. In contrast, both cAT3G5Cs DME10 and ATMSCs had the pathway terms ''ECM-receptor interaction,'' ''focal adhesion,'' and ''pathways in cancer,'' over-represented when compared with cAT3G5Cs, which once again reinforces the similarities between cAT3G5Cs DME10 and ATMSCs.

FIG. 5. Immunophenotype of freshly isolated AT3G5Cs. Plastic adherent $3G5^{+}CD31^{-}$ cells (AT3G5Cs) were isolated from human subcutaneous adipose tissue from two different donors by fluorescence-activated cell sorting, and double-immunostained with antibodies to detect the molecules indicated, or with control antibodies (IgG). **(A)** Dot plots of AT3G5Cs from donor no. 19. Expression of NG2 is additionally shown as a histogram (*solid line*) plotted against a control histogram (*shaded*). **(B)** Dot plots of AT3G5Cs from donor no. 20. NG2, nerve/glial antigen 2.

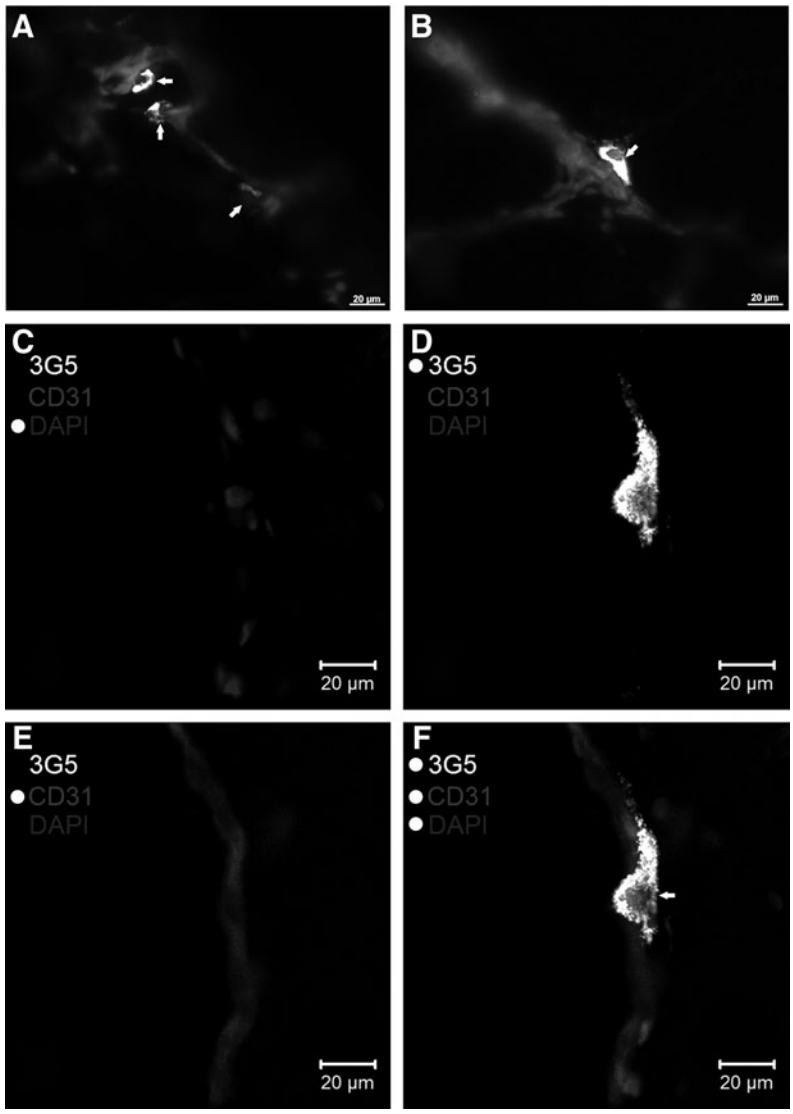

FIG. 6. Immunodetection of $3G5^{+}CD31^{-}$ cells in situ. Cryosections of subcutaneous adipose tissue were stained with an anti-CD31 antibody to identify endothelial cells and with the 3G5 antibody to identify pericytes. **(A, B)** Micrographs of sections observed using standard fluorescence microscopy; *arrows* indicate $3G5^{+}$ cells. **(C–F)** Sequence of confocal microscopy micrographs showing nuclei stained with DAPI **(C)**, a $3G5^{+}$ cell **(D)**, a microvessel **(E)**, and a composite image **(F)**, with an *arrow* indicating the $3G5^{+}$ cell. DAPI, 4′,6-diamidino-2-phenylindole.

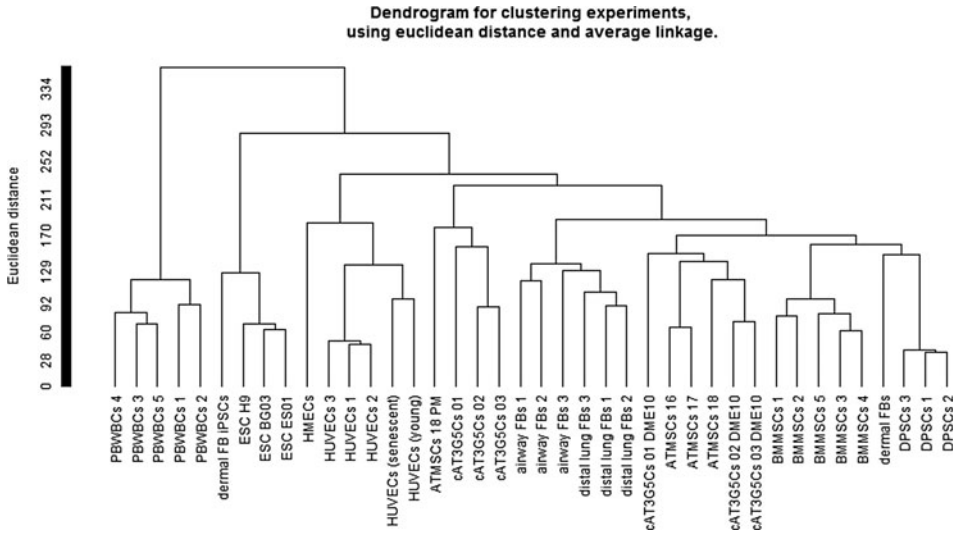

FIG. 7. Hierarchical clustering of cAT3G5Cs, ATMSCs, and other cell types. Microarray data were clustered using Euclidean distance with average linkage. airway FBs, airway fibroblasts; ATMSCs 18 PM, ATMSCs from donor no. 18 cultured in pericyte medium; cAT3G5Cs, adipose tissue-derived $3G5^{+}$ cells cultured in pericyte medium; cAT3G5Cs DME10, cAT3G5Cs cultured in ATMSC medium (DMEM + 10% fetal bovine serum); dermal FB iPSCs, dermal fibroblast induced pluripotent stem cells; dermal FBs, dermal fibroblasts; distal lung FBs, distal lung fibroblasts; DMEM, Dulbecco's modified Eagle's medium; ESC, embryonic stem cell (additional letters designate specific cell lines); HMECs, human microvascular endothelial cells; PBWBCs, peripheral blood white blood cells (numbers indicate different samples).

Table 2. Genes Differentially Expressed by cAT3G5Cs DME10 or ATMSCs Compared With Each Other

cAT3G5Cs DME10				*ATMSCs*							
Symbol	*Fold-change*	*Parametric P value*	*FDR*	*Symbol*	*Fold-change*	*Parametric P value*	*FDR*	*Symbol*	*Fold-change*	*Parametric P value*	*FDR*
SCN9A	47.62	1.59E-05	0.00984	*SFRP2*	562.05	1.20E-06	0.00445	*GALNAC4S-6ST*	11.86	0.000495	0.0596
COL4A5	45.45	1.25E-05	0.00935	*FAM19A5*	505.13	<1e-07	<1e-07	*LARGE*	11.78	5.87E-05	0.0198
SCN9A	38.46	2.10E-06	0.00495	*SMOC2*	388.47	2.30E-06	0.00495	*RAI2*	11.60	0.000501	0.06
IGF2BP3	37.04	0.000136	0.0291	*H19*	181.93	1.55E-05	0.00984	*HTRA3*	10.88	0.000639	0.0678
GALNT3	34.48	2.13E-05	0.0116	*MYH11*	160.04	1.58E-05	0.00984	***VWF***	10.43	0.000245	0.0398
EREG	33.33	0.000156	0.0311	*SYNDIG1*	125.69	8.10E-06	0.00742	*RSPO3*	10.02	0.000262	0.0413
DNER	33.33	0.00068	0.069	*LYPD6*	101.74	4.00E-06	0.0053	*MALL*	9.92	0.000796	0.0737
FOXF1	22.22	0.000391	0.0527	*SLC24A3*	75.21	1.31E-05	0.00935	*GPRC5C*	9.35	2.69E-05	0.0136
MYPN	20.00	0.000905	0.0789	*IGF1*	72.54	4.25E-05	0.0168	*BCL6B*	9.22	3.80E-06	0.0053
HIVEP3	18.18	4.19E-05	0.0168	*COMP*	71.61	0.000182	0.0342	*PLXDC1*	8.90	0.000121	0.0277
IGF2BP1	16.67	0.000111	0.0268	*IGF1*	71.25	2.55E-05	0.0135	*LOC400456*	8.68	1.27E-05	0.00935
NTF4	15.38	7.00E-06	0.00684	*GDF10*	68.83	3.70E-06	0.0053	*PDE10A*	8.52	3.21E-05	0.0149
RUNX1–IT1	14.49	0.000122	0.0277	*TRH*	67.65	1.66E-05	0.00994	*HOMER2*	8.48	0.000137	0.0291
CPA4	14.49	0.000222	0.0382	*MYH11*	66.43	6.11E-05	0.0199	***TIE1***	8.38	0.000274	0.0424
ELFN2	13.33	0.000787	0.0737	*GRID1*	65.31	2.89E-05	0.0141	***ECSM2***	8.17	0.000377	0.0519
GLIS1	13.16	1.79E-05	0.0101	*LSP1*	59.09	8.73E-05	0.0235	*ZNF385D*	8.06	0.00047	0.0578
LTBP1	12.05	0.000947	0.0805	*RSPO3*	53.47	0.000247	0.0398	*ADCY1*	8.01	0.00066	0.0685
GDNF	11.36	0.000933	0.0805	*EFS*	52.99	3.34E-05	0.015	*CHRDL1*	7.92	0.000312	0.0459
ADAMTS16	10.53	0.000895	0.0789	*APCDD1*	52.84	1.09E-05	0.0092	*DOCK8*	7.87	0.000629	0.0676
IL8	10.00	0.000463	0.0577	*FNDC1*	51.38	0.000109	0.0265	*GNAO1*	7.73	0.000346	0.0491
FGF5	10.00	0.000634	0.0676	*CXCR4*	50.87	7.30E-05	0.0207	*FAM70A*	7.66	7.34E-05	0.0207
DIRAS3	9.09	4.90E-05	0.0186	*SCARA5*	48.47	0.000786	0.0737	***KDR***	7.63	9.12E-05	0.0238
EVI1	9.09	8.49E-05	0.0232	*WNT2*	47.22	0.000287	0.0432	*IRX4*	7.62	0.000215	0.0379
SRGN	9.09	0.000178	0.0338	*CCDC3*	46.72	3.79E-05	0.016	*CYP26B1*	7.33	4.63E-05	0.0179
LIN7A	9.09	0.00055	0.0639	*ITGA8*	46.33	8.00E-07	0.00445	*TM4SF18*	7.18	0.000137	0.0291
FLJ35409	8.33	0.000469	0.0578	*CLIC6*	38.71	0.000694	0.069	*SEMA3D*	7.11	0.000429	0.0554
MAP3K5	8.33	0.000759	0.0726	*STAB1*	32.46	0.000662	0.0685	*ELN*	6.89	0.000942	0.0805
FRMPD4	7.69	0.000105	0.0259	*ROR2*	32.39	9.45E-05	0.024	*PDE1C*	6.88	0.00076	0.0726
FRMPD4	7.69	0.000594	0.0668	***LIPG***	31.20	1.49E-05	0.00984	*RASGRP3*	6.77	0.000592	0.0668
GRAMD1C	7.14	3.39E-05	0.015	*TSHZ2*	30.72	8.40E-06	0.00742	*LASS4*	6.77	0.000812	0.0742
PIANP	7.14	0.000151	0.0306	*GUCY1A2*	27.59	3.00E-07	0.00278	*CAMK1D*	6.73	0.000127	0.0281
LOC440338	7.14	0.000432	0.0554	***PECAM1***	26.87	0.000221	0.0382	*FMO3*	6.45	0.000412	0.0547
BIRC3	6.67	0.00023	0.0388	*ACAN*	26.22	0.000143	0.0298	*STK32B*	6.41	3.96E-05	0.0163
FBXL16	6.67	0.000668	0.0685	*AQP1*	25.14	7.20E-05	0.0207	*PCDHB4*	6.36	0.00021	0.0376
HS6ST3	6.25	1.19E-05	0.00935	*LDLRAD4*	24.80	2.40E-06	0.00495	*SOX17*	6.18	0.000432	0.0554
RAGE	6.25	5.83E-05	0.0198	*LINGO2*	24.63	5.76E-05	0.0198	*SHE*	6.11	0.000341	0.0488
NCAM2	6.25	0.000606	0.0674	*LMO2*	24.61	0.000138	0.0291	*FMOD*	6.06	0.000682	0.069
ADAM23	5.88	7.37E-05	0.0207	*AIF1L*	23.95	0.000515	0.0608	*PCDHAC2*	5.63	2.71E-05	0.0136
IL15	5.88	0.000217	0.0379	*EMCN*	22.86	0.000121	0.0277	*A2M*	5.40	7.03E-05	0.0207
TNFSF14	5.56	0.000852	0.0769	*ACTG2*	22.72	0.00036	0.0498	*KCNA1*	5.37	0.000115	0.0273

(*continued*)

TABLE 2. (CONTINUED)

cAT3G5Cs DME10				*ATMSCs*							
Symbol	*Fold-change*	*Parametric* P *value*	*FDR*	*Symbol*	*Fold-change*	*Parametric* P *value*	*FDR*	*Symbol*	*Fold-change*	*Parametric* P *value*	*FDR*
SMOC1	5.26	0.000211	0.0376	*CNTN1*	22.67	0.000101	0.0254	*PLXDC1*	5.36	0.00079	0.0737
LOC129293	5.00	0.000152	0.0306	*TNNT3*	22.55	5.90E-06	0.00684	*GIMAP6*	5.35	5.20E-05	0.0191
F2RL2	5.00	0.000228	0.0388	*LL22NC03-75B3.6*	21.76	0.000206	0.0375	*CAMK1D*	5.30	0.000358	0.0498
B3GNT5	5.00	0.000328	0.0479	*EFHD1*	21.65	3.66E-05	0.0158	*PTPRN*	5.25	0.000876	0.0785
WDR63	5.00	0.000392	0.0527	*ADRA2A*	21.25	2.30E-06	0.00495	*CDS1*	5.23	0.000485	0.0588
PER1	4.76	0.000163	0.0319	*COL6A6*	21.19	6.40E-06	0.00684	*FAM124A*	5.20	0.000648	0.0683
PLEKHG5	4.76	0.000583	0.0664	*NTF3*	20.72	0.000463	0.0577	*RICH2*	5.05	0.000827	0.0753
CLGN	4.55	5.48E-05	0.0196	*FLJ11235*	19.98	1.00E-06	0.00445	*FGFR2*	5.04	0.000763	0.0726
KLHL3	4.55	0.000392	0.0527	*CNGA3*	19.66	0.000152	0.0306	*FBP1*	5.02	0.000603	0.0674
WDR66	4.55	0.000798	0.0737	*SORBS1*	19.43	6.90E-06	0.00684	*PLEKHG1*	4.82	0.000119	0.0277
SAMD13	4.35	5.24E-05	0.0191	*PDLIM3*	19.15	0.000355	0.0498	*SORCS2*	4.82	0.000759	0.0726
DNAH7	4.35	0.00048	0.0586	*C10orf58*	18.49	3.18E-05	0.0149	*FAM149A*	4.77	0.000906	0.0789
RELB	4.00	7.92E-05	0.0219	*EPB41L4A*	17.37	6.72E-05	0.0207	*KCND3*	4.68	0.000736	0.0719
PAPLN	4.00	0.000276	0.0424	*HSPA12B*	16.62	0.000125	0.028	*LRRC4C*	4.41	7.01E-05	0.0207
SOX5	3.70	0.000165	0.0319	*RBPMS2*	15.78	0.000283	0.0431	*ENPP5*	4.40	0.000342	0.0488
IRS2	3.70	0.000176	0.0336	*KANK4*	15.74	0.000752	0.0726	*C1orf106*	4.34	0.000265	0.0413
PLEC1	3.70	0.000459	0.0577	*OLFM4*	15.48	0.000525	0.0616	*ACVR2A*	4.23	0.000334	0.0484
SLC16A6	3.70	0.000721	0.0711	*PDZRN4*	15.47	0.000415	0.0547	*LOC645427*	4.09	0.000574	0.0657
ZNF154	3.57	0.000613	0.0675	*LAPTM5*	15.03	0.000252	0.0403	*ATL1*	4.00	0.000234	0.0391
PLEKHH2	3.57	0.000898	0.0789	*MEOX2*	14.94	8.85E-05	0.0235	*OLFML1*	3.93	0.000185	0.0342
KBTBD8	3.33	0.000433	0.0554	*ALDH1A1*	14.49	0.000238	0.0391	*FLJ22662*	3.87	0.000289	0.0432
CXorf57	3.33	0.000993	0.083	*NPY1R*	14.34	3.10E-06	0.0053	*SGK493*	3.84	0.000922	0.08
LOC100130924	3.23	0.000664	0.0685	*FAM65B*	14.28	0.000615	0.0675	*CYP26A1*	3.79	0.00069	0.069
WNT5B	3.13	0.000688	0.069	*CPVL*	13.77	0.000955	0.0805	*PLXNC1*	3.76	0.000625	0.0676
CHML	3.13	0.000806	0.074	*COCH*	13.68	6.85E-05	0.0207	*BMP7*	3.68	0.000265	0.0413
PTPRK	3.03	0.000731	0.0718	*ALOX5*	13.61	9.27E-05	0.0239	*FOLH1*	3.53	0.000953	0.0805
DRAM	2.94	0.000505	0.0601	*LSAMP*	13.60	6.12E-05	0.0199	*NOTCH4*	3.46	0.000416	0.0547
DEF6	2.94	0.000887	0.0787	*PTPRN2*	13.50	1.74E-05	0.0101	*NDN*	3.09	0.000663	0.0685
KIAA1598	2.94	0.000948	0.0805	*DDIT4L*	13.21	6.40E-05	0.0205	*NGF*	3.06	0.00098	0.0823
FZD7	2.78	0.000437	0.0556	*KIT*	13.06	0.000195	0.0359	*GPR4*	2.99	0.00063	0.0676
TOM1L1	2.78	0.00056	0.0646	*PCSK1*	12.95	0.000238	0.0391	*GIMAP8*	2.73	0.000551	0.0639
UCA1	2.78	0.000854	0.0769	*RRAGD*	12.59	6.80E-06	0.00684	*NHEJ1*	2.67	0.000695	0.069
KIR3DL3	2.70	0.000619	0.0676	*LOC54492*	12.34	0.000165	0.0319				
HIPK2	2.70	0.000796	0.0737	***CD93***	12.10	3.20E-06	0.0053				
CPEB2	2.63	0.000881	0.0786	*PGM5*	11.88	0.000302	0.0449				

After differential expression analysis, transcripts were ranked as per fold-change values. Endothelial cell-specific transcripts are highlighted in *bold*.

ATMSCs, adipose tissue-derived mesenchymal stromal cells; cAT3G5Cs DME10, adipose tissue-derived $3G5^{+}CD31^{-}$ cells cultured in DMEM with 10% fetal bovine serum; FDR, false detection rate.

Table 3. Pathway Analysis of Genes Significantly Upregulated in cAT3G5Cs, cAT3G5Cs DME10, and ATMSCs

KEGG term	*Count*	*%*	P *value*	*Benjamini*
Transcripts upregulated in cAT3G5Cs DME10 compared with ATMSCs				
hsa05200:pathways in cancer	6	8.33	0.005933	0.197633
hsa04010:MAPK signaling pathway	5	6.94	0.015412	0.249743
hsa04722:neurotrophin signaling pathway	3	4.17	0.077016	0.627844
Transcripts upregulated in ATMSCs compared with cAT3G5Cs DME10				
hsa04510:focal adhesion	6	4.23	0.039665	0.924999
hsa04512:ECM-receptor interaction	4	2.82	0.044163	0.764343
hsa04916:melanogenesis	4	2.82	0.065976	0.766848
hsa04270:vascular smooth muscle contraction	4	2.82	0.08818	0.77168
hsa00830:retinol metabolism	3	2.11	0.09163	0.707745
Transcripts upregulated in cAT3G5Cs compared with cAT3G5Cs DME10				
hsa03030:DNA replication	23	2.37	4.10E-19	6.24E-17
hsa04110:cell cycle	32	3.30	1.17E-12	8.91E-11
hsa00240:pyrimidine metabolism	21	2.16	2.69E-07	1.36E-05
hsa00230:purine metabolism	26	2.68	1.44E-06	5.45E-05
hsa03430:mismatch repair	10	1.03	2.40E-06	7.31E-05
hsa03410:base excision repair	9	0.93	6.47E-04	0.016267
hsa03420:nucleotide excision repair	10	1.03	7.15E-04	0.015419
hsa03020:RNA polymerase	8	0.82	7.97E-04	0.015032
hsa00900:terpenoid backbone biosynthesis	6	0.62	0.001124	0.018813
Transcripts upregulated in cAT3G5Cs DME10 compared with cAT3G5Cs				
hsa04512:ECM-receptor interaction	16	1.74	5.39E-06	7.49E-04
hsa04510:focal adhesion	24	2.60	4.53E-05	0.003144
hsa05200:pathways in cancer	30	3.25	5.02E-04	0.023019
Transcripts upregulated in cAT3G5Cs compared with ATMSCs				
hsa03030:DNA replication	22	1.91	4.00E-16	7.37E-14
hsa04110:cell cycle	33	2.87	2.41E-11	2.00E-09
hsa03430:mismatch repair	10	0.87	1.03E-05	5.69E-04
hsa00240:pyrimidine metabolism	20	1.74	1.66E-05	6.89E-04
hsa00230:purine metabolism	24	2.09	2.48E-04	0.008206
hsa03420:nucleotide excision repair	11	0.96	6.01E-04	0.016502
hsa03410:base excision repair	9	0.78	0.002034	0.047126
hsa03440:homologous recombination	8	0.70	0.002232	0.045299
hsa00900:terpenoid backbone biosynthesis	6	0.52	0.00247	0.044587
Transcripts upregulated in ATMSCs compared with cAT3G5Cs				
hsa04512:ECM-receptor interaction	21	1.75	1.08E-07	1.73E-05
hsa04510:focal adhesion	33	2.75	4.85E-07	3.90E-05
hsa05200:pathways in cancer	37	3.08	4.45E-04	0.023602

Genes upregulated in cAT3G5Cs, cAT3G5Cs DME10, and ATMSCs were analyzed using the Functional Annotation Tool in DAVID, with *Homo sapiens* selected as the background. Genes that are involved in the indicated KEGG pathway terms are listed. Count, number of genes that match the indicated pathway term; %, percentage of genes relative to the total number of genes involved in the indicated pathway; *P* value, parametric *P* value; Benjamini, *P* value as adjusted using the Benjamini–Hochberg method. In the absence of significant pathway over-representation in the cAT3G5Cs DME10 versus ATMSC analysis, all resultant terms are shown. Only terms significantly over-represented are listed for the cAT3G5Cs versus cAT3G5Cs and cAT3G5Cs versus ATMSCs analyses.

ECM, extracellular matrix; KEGG, Kyoto Encyclopedia of Genes and Genomes.

Discussion

The antigen defined by the 3G5 antibody has been validated as a PC marker in several studies [10–12,30]. Marker molecules exhibit specific identification of their target cells only in specific contexts. The 3G5 antibody has been shown to specifically detect the 3G5 antigen on the surface of PCs in the vasculature as other cell types, such as neuroendocrine cells [31], a subpopulation of T cells [32], kidney tubular cells [33], melanocytes [34], and keratocytes [35], also express this antigen on their surface. Gushi et al. [36] reported detection of the 3G5 antigen in the granules–but not on the surface–of mast cells in human skin, but overlooked the fact that antibodies can nonspecifically bind to mast cell granules [37]. All of these details regarding the identification of cells by the 3G5 antibody highlight the importance of the methodology used to isolate PCs in this study as the cells selected by us (1) were derived from the AT SVF, which greatly reduces the possibility of staining of cells not associated with the vasculature; (2) were plastic adherent, which means nonadherent cells such as T cells were discarded before immunostaining; (3) expressed the 3G5 antigen on their surface, as required for FACS; and (4) did not express CD31, which ensures ECs, or other $CD31^+$ cells, physically attached to PCs were excluded. The cells obtained through this methodology (AT3G5Cs) are periendothelial in situ, and express the PC markers, 3G5 and CD140b, whereas the cultured cells derived from them (cAT3G5Cs)

express PC-associated molecules, such as CD140b and CD13, in addition to the activated PC marker, NG2. In this context, it is reasonable to regard AT3G5Cs as PCs.

According to the hypothesis that PCs give rise to MSC cultures [5], cAT3G5Cs should share functional properties and surface molecule profile with MSCs. In line with this, the surface imunophenotypes or cAT3G5Cs and ATMSCs were essentially identical, and both cell types exhibited a similar ability to inhibit the proliferation of peripheral blood $CD3^+$ cells in direct contact coculture. It is noteworthy that cAT3G5Cs lose expression of the 3G5 antigen when expanded in culture and become $3G5^-$ as ATMSCs.

Studies in which $3G5^+$ cells were isolated and had 3G5 expression reassessed after culture expansion are scarce. Helmbold et al. [38] reported maintenance of the 3G5 antigen in dermal PCs cultured on type I collagen in medium containing 10% bovine retinal EC culture supernatant. Expression of the 3G5 antigen in human corneal keratocytes is lost in culture, but can be reacquired after treatment with transforming growth factor-β [35]. It is possible that the conditions used by us favor acquisition of an activated PC phenotype by AT3G5Cs as cAT3G5Cs express appreciable levels of the activated PC marker, NG2, on their surface, but lack expression of the 3G5 antigen. The possibility that cAT3G5Cs reexpress the 3G5 antigen when cultured in conditions that closely mimic the native PC environment was not tested in this study and cannot be discarded.

Differences between cAT3G5Cs and ATMSCs were also found. During differentiation experiments, the osteogenic and adipogenic differentiation efficiencies of cAT3G5Cs were far superior to those exhibited by ATMSCs. The purpose of these differentiation assays was to verify that cAT3G5Cs exhibit the in vitro differentiation potential required to be considered MSCs, while ATMSCs were used as controls. Therefore, investigating the causes of the in vitro differentiation ability differences between cAT3G5Cs and ATMSCs was beyond the scope of this study.

It is possible that the discrepancies found between cAT3G5Cs and ATMSCs are a consequence of the conditions used to establish the cultures and expand the cells. Various cell types are present during the establishment of MSC cultures, which are maintained in basal medium containing 10% FBS; conversely, AT3G5Cs establish long-term cultures in the absence of other cell types and are maintained in basal medium that contains 2% FBS. On the other hand, in view of the presence of RNAs that code for EC makers in ATMSCs, it is possible that small amounts of ECs in these cultures negatively interfere with differentiation in a manner similar to that described by Rajashekhar et al. [39], who showed impaired adipogenic differentiation of ATMSCs when in the presence of ECs. Since ECs are not detectable by flow cytometry in ATMSC cultures, we speculate that the sources of EC-specific transcripts in ATMSCs are ECs that underwent endothelial-to-mesenchymal transition [40] during culture establishment.

Differences apart, similarities between cAT3G5Cs and ATMSCs prevail when the former are cultured under ATMSC conditions, as shown by gene expression profile clustering experiments, in which three cAT3G5C populations clustered with ATMSCs when cultured in MSC medium. Similarities between cAT3G5Cs and ATMSCs are further emphasized by the fact that an ATMSC population cultured in PM clusters with cAT3G5Cs cultured in PM. The gene expression analyses described here indicate that PCs change their phenotype in culture to become MSCs. Altogether, our results indicate that cAT3G5Cs represent MSCs established in the absence of cell types such as ECs, which strengthens the hypothesis that the progeny of PCs contribute to MSC cultures.

Recently, Kramann et al. [41] reported a population of murine perivascular $Gli1^+$ cells that express the antigen defined by the 3G5 antigen, but do not express significant levels of CD146 or NG2 in situ, just like AT3G5Cs. These $Gli1^+$ cells were reported to give rise to MSC cultures and acquire expression of CD146 and NG2. Since AT3G5Cs give rise to cells that express CD146 and NG2 in culture, they could correspond to human counterparts of the $Gli1^+$ cells described by Kramann et al. [41].

Friedenstein proposed that fibroblast colony-forming units (CFU-Fs) give rise to stromal cultures [42], and Owen proposed that CFU-Fs encompass stromal stem cells and committed precursors [43]. The results shown here suggest PCs represent primordial CFU-Fs, while $CD146^+$ perivascular cells represent progenitors ultimately derived from PCs. This view could explain the establishment of MSC cultures by AT3G5Cs as shown here and by $CD146^+CD56^-$ perivascular cells in various organs [8], including skeletal muscle [44].

Acknowledgments

The authors are indebted to the team of Divisão de Cirurgia Plástica e Queimaduras of Hospital das Clínicas de Ribeirão Preto for providing AT samples and Ms. Aline Magro Bueno for technical assistance. The P2B1 hybridoma developed by Elizabeth A. Wayner and Gregory Vercellotti was obtained from the Developmental Studies Hybridoma Bank developed under the auspices of the NICHD and maintained by the University of Iowa, Department of Biology, Iowa City, IA. This work has been funded by the following grants: #2013/08135-2, São Paulo Research Foundation (FAPESP); USP #12.1.25441.01.2, Research Support of the University of São Paulo, CISBi-NAP; and grants #477806/2008-2, #573754/2008-0, and #131371/2011-8, Brazilian National Council for Scientific and Technological Development (CNPq).

Author Disclosure Statement

The institutions involved in this work (Fundação Hemocentro de Ribeirão Preto and University of São Paulo) have jointly applied for a patent on the methodology used for PC isolation at the Brazilian National Institute for Intellectual Property, with L.da S.M. and D.T.C listed as inventors. The results presented in the article serve solely scientific purposes.

References

1. Caplan AI. (1991). Mesenchymal stem cells. J Orthop Res 9:641–650.
2. Dominici M, K Le Blanc, I Mueller, I Slaper-Cortenbach, F Marini, D Krause, R Deans, A Keating, D Prockop and E Horwitz. (2006). Minimal criteria for defining multipotent mesenchymal stromal cells. The International Society for Cellular Therapy position statement. Cytotherapy 8:315–317.

3. Caplan AI and SP Bruder. (2001). Mesenchymal stem cells: building blocks for molecular medicine in the 21st century. Trends Mol Med 7:259–264.
4. Meirelles Lda S, AM Fontes, DT Covas and AI Caplan. (2009). Mechanisms involved in the therapeutic properties of mesenchymal stem cells. Cytokine Growth Factor Rev 20:419–427.
5. da Silva Meirelles L, AI Caplan and NB Nardi. (2008). In search of the in vivo identity of mesenchymal stem cells. Stem Cells 26:2287–2299.
6. Geevarghese A and IM Herman. (2014). Pericyte-endothelial crosstalk: implications and opportunities for advanced cellular therapies. Transl Res 163:296–306.
7. Bardin N, F George, M Mutin, C Brisson, N Horschowski, V Frances, G Lesaule and J Sampol. (1996). S-Endo 1, a pan-endothelial monoclonal antibody recognizing a novel human endothelial antigen. Tissue Antigens 48:531–539.
8. Crisan M, S Yap, L Casteilla, CW Chen, M Corselli, TS Park, G Andriolo, B Sun, B Zheng, et al. (2008). A perivascular origin for mesenchymal stem cells in multiple human organs. Cell Stem Cell 3:301–313.
9. Zuk PA, M Zhu, H Mizuno, J Huang, JW Futrell, AJ Katz, P Benhaim, HP Lorenz and MH Hedrick. (2001). Multilineage cells from human adipose tissue: implications for cell-based therapies. Tissue Eng 7:211–228.
10. Helmbold P, J Wohlrab, WC Marsch and RC Nayak. (2001). Human dermal pericytes express 3G5 ganglioside—a new approach for microvessel histology in the skin. J Cutan Pathol 28:206–210.
11. Nayak RC, AB Berman, KL George, GS Eisenbarth and GL King. (1988). A monoclonal antibody (3G5)-defined ganglioside antigen is expressed on the cell surface of microvascular pericytes. J Exp Med 167:1003–1015.
12. Zannettino AC, S Paton, A Arthur, F Khor, S Itescu, JM Gimble and S Gronthos. (2008). Multipotential human adipose-derived stromal stem cells exhibit a perivascular phenotype in vitro and in vivo. J Cell Physiol 214:413–421.
13. Garlanda C and E Dejana. (1997). Heterogeneity of endothelial cells. Specific markers. Arterioscler Thromb Vasc Biol 17:1193–1202.
14. Lennon DP and AI Caplan. (2006). Isolation of human marrow-derived mesenchymal stem cells. Exp Hematol 34: 1604–1605.
15. Johnstone B, TM Hering, AI Caplan, VM Goldberg and JU Yoo. (1998). In vitro chondrogenesis of bone marrow-derived mesenchymal progenitor cells. Exp Cell Res 238: 265–272.
16. Mackay AM, SC Beck, JM Murphy, FP Barry, CO Chichester and MF Pittenger. (1998). Chondrogenic differentiation of cultured human mesenchymal stem cells from marrow. Tissue Eng 4:415–428.
17. Royer-Pokora B, M Busch, M Beier, C Duhme, C de Torres, J Mora, A Brandt and HD Royer. (2010). Wilms tumor cells with WT1 mutations have characteristic features of mesenchymal stem cells and express molecular markers of paraxial mesoderm. Hum Mol Genet 19:1651–1668.
18. Takahashi K and S Yamanaka. (2006). Induction of pluripotent stem cells from mouse embryonic and adult fibroblast cultures by defined factors. Cell 126:663–676.
19. Zhou X, W Wu, H Hu, J Milosevic, K Konishi, N Kaminski and SE Wenzel. (2011). Genomic differences distinguish the myofibroblast phenotype of distal lung fibroblasts from airway fibroblasts. Am J Respir Cell Mol Biol 45:1256–1262.
20. van Balkom BW, OG de Jong, M Smits, J Brummelman, K den Ouden, PM de Bree, MA van Eijndhoven, DM Pegtel, W Stoorvogel, T Wurdinger and MC Verhaar. (2013). Endothelial cells require miR-214 to secrete exosomes that suppress senescence and induce angiogenesis in human and mouse endothelial cells. Blood 121:3997–4006, S1–S15.
21. Conway DE, MR Williams, SG Eskin and LV McIntire. (2010). Endothelial cell responses to atheroprone flow are driven by two separate flow components: low time-average shear stress and fluid flow reversal. Am J Physiol Heart Circ Physiol 298:H367–H374.
22. Jong HL, MR Mustafa, PM Vanhoutte, S AbuBakar and PF Wong. (2013). MicroRNA 299-3p modulates replicative senescence in endothelial cells. Physiol Genomics 45:256–267.
23. Tesar PJ, JG Chenoweth, FA Brook, TJ Davies, EP Evans, DL Mack, RL Gardner and RD McKay. (2007). New cell lines from mouse epiblast share defining features with human embryonic stem cells. Nature 448:196–199.
24. Nakamura S, M Kobayashi, T Sugino, O Kajimoto, R Matoba and K Matsubara. (2010). Effect of exercise on gene expression profile in unfractionated peripheral blood leukocytes. Biochem Biophys Res Commun 391:846–851.
25. Ahn SJ, JH Jang, JS Seo, KM Cho, SH Jung, HW Lee, EC Kim and SH Park. (2013). Influence of 2 cryopreservation methods to induce CCL-13 from dental pulp cells. J Endod 39:1562–1566.
26. Dellavalle A, M Sampaolesi, R Tonlorenzi, E Tagliafico, B Sacchetti, L Perani, A Innocenzi, BG Galvez, G Messina, et al. (2007). Pericytes of human skeletal muscle are myogenic precursors distinct from satellite cells. Nat Cell Biol 9:255–267.
27. Boneberg EM, H Illges, DF Legler and G Furstenberger. (2009). Soluble CD146 is generated by ectodomain shedding of membrane CD146 in a calcium-induced, matrix metalloprotease-dependent process. Microvasc Res 78: 325–331.
28. Schlingemann RO, FJ Rietveld, RM de Waal, S Ferrone and DJ Ruiter. (1990). Expression of the high molecular weight melanoma-associated antigen by pericytes during angiogenesis in tumors and in healing wounds. Am J Pathol 136:1393–1405.
29. Varma MJ, RG Breuls, TE Schouten, WJ Jurgens, HJ Bontkes, GJ Schuurhuis, SM van Ham and FJ van Milligen. (2007). Phenotypical and functional characterization of freshly isolated adipose tissue-derived stem cells. Stem Cells Dev 16:91–104.
30. Shi S and S Gronthos. (2003). Perivascular niche of postnatal mesenchymal stem cells in human bone marrow and dental pulp. J Bone Miner Res 18:696–704.
31. Powers AC, A Rabizadeh, R Akeson and GS Eisenbarth. (1984). Characterization of monoclonal antibody 3G5 and utilization of this antibody to immobilize pancreatic islet cell gangliosides in a solid phase radioassay. Endocrinology 114:1338–1343.
32. Rabinowe SL, RC Nayak, K Krisch, KL George and GS Eisenbarth. (1987). Aging in man. Linear increase of a novel T cell subset defined by antiganglioside monoclonal antibody 3G5. J Exp Med 165:1436–1441.
33. Nayak RC, MA Attawia, CJ Cahill, GL King, H Ohashi and R Moromisato. (1992). Expression of a monoclonal anti-

body (3G5) defined ganglioside antigen in the renal cortex. Kidney Int 41:1638–1645.
34. Fiedler E, RC Nayak, W Marsch and P Helmbold. (2004). Melanocytes express 3G5 surface antigen. Am J Dermatopathol 26:200–204.
35. Stramer BM, MG Kwok, PJ Farthing-Nayak, JC Jung, ME Fini and RC Nayak. (2004). Monoclonal antibody (3G5)-defined ganglioside: cell surface marker of corneal keratocytes. Invest Ophthalmol Vis Sci 45:807–812.
36. Gushi A, M Tanaka, S Tsuyama, T Nagai, T Kanzaki, T Kanekura and T Matsuyama. (2008). The 3G5 antigen is expressed in dermal mast cells but not pericytes. J Cutan Pathol 35:278–284.
37. Schiltz PM, J Lieber, RC Giorno and HN Claman. (1993). Mast cell immunohistochemistry: non-immunological immunostaining mediated by non-specific F(ab′)2-mast cell secretory granule interaction. Histochem J 25:642–647.
38. Helmbold P, RC Nayak, WC Marsch and IM Herman. (2001). Isolation and in vitro characterization of human dermal microvascular pericytes. Microvasc Res 61:160–165.
39. Rajashekhar G, DO Traktuev, WC Roell, BH Johnstone, S Merfeld-Clauss, B Van Natta, ED Rosen, KL March and M Clauss. (2008). IFATS collection: Adipose stromal cell differentiation is reduced by endothelial cell contact and paracrine communication: role of canonical Wnt signaling. Stem Cells 26:2674–2681.
40. Medici D, EM Shore, VY Lounev, FS Kaplan, R Kalluri and BR Olsen. (2010). Conversion of vascular endothelial cells into multipotent stem-like cells. Nat Med 16:1400–1406.
41. Kramann R, RK Schneider, DP DiRocco, F Machado, S Fleig, PA Bondzie, JM Henderson, BL Ebert and BD Humphreys. (2015). Perivascular Gli1 + progenitors are key contributors to injury-induced organ fibrosis. Cell Stem Cell 16:51–66.
42. Friedenstein AJ, RK Chailakhjan and KS Lalykina. (1970). The development of fibroblast colonies in monolayer cultures of guinea-pig bone marrow and spleen cells. Cell Tissue Kinet 3:393–403.
43. Owen M. (1988). Marrow stromal stem cells. J Cell Sci Suppl 10:63–76.
44. Chen WC, A Saparov, M Corselli, M Crisan, B Zheng, B Peault and J Huard. (2014). Isolation of blood-vessel-derived multipotent precursors from human skeletal muscle. J Vis Exp e51195.

Address correspondence to:
Dr. Lindolfo da Silva Meirelles
Laboratory for Stem Cells and Tissue Engineering
PPGBioSaúde
Lutheran University of Brazil
Av. Farroupilha 8001
Canoas 92425-900
Rio Grande do Sul
Brazil

E-mail: lindolfomeirelles@gmail.com
lindolfomeirelles@ulbra.edu.br

Received for publication April 24, 2015
Accepted after revision July 17, 2015
Prepublished on Liebert Instant Online July 20, 2015